LA-8223-MS

Informal Report

2

Space Nuclear Reactor Power Plants

University of California

LOS ALAMOS SCIENTIFIC LABORATORY

Post Office Box 1663   Los Alamos. New Mexico 87545

This report was not edited by the Technical
Information staff.

**UNITED STATES
DEPARTMENT OF ENERGY
CONTRACT W-7405-ENG. 36**

Space Nuclear Reactor Power Plants

D. Buden
W. A. Ranken
D. R. Koenig

CONTENTS

SPACE NUCLEAR REACTOR POWER PLANTS

by

D. Buden
W. A. Ranken
D. R. Koenig

ABSTRACT

Requirements for electrical and propulsion power
for space are expected to increase dramatically in
the 1980s. Nuclear power is probably the only
source for some deep space missions and a major
competitor for many orbital missions, especially
those at geosynchronous orbit. Because of the
potential requirements, a technology program on
space nuclear power plant components has been
initiated by the Department of Energy. The mis-
sions that are foreseen, the current power plant
concept, the technology program plan, and early
key results are described.

I. POTENTIAL MISSION REQUIREMENTS[1]

When the Space Transportation System (STS) be-
comes operational we will enter a new era in space
exploration and exploitation, one that will lead to
increasingly complex large space satellites. Many
of the great advances in space we have seen to date
will be like the early biplanes compared to today's
747 jet liners. There are a number of key technol-
ogies emerging that will make this new era feasible,
including new approaches of meeting vastly increased
demands for power. Large quantities of electrical
power will be needed for both sensors and propul-
sion. Since we will be discussing the potential use
of nuclear power, we will concentrate on those areas
that appear most attractive for nuclear power, i.e.,
high-power satellites in geosynchronous orbit and
electric propulsion systems for both orbital trans-
fer and planetary exploration missions.

A. Potential Security Applications

To understand why we consider reactors a neces-
sity for space electrical power, one should have an
understanding of the role space will play in future
national defense. The statement -- "take the high
ground and hold it" -- is recognized as axiomatic in
defense. But, where will the "high ground" be in
the future? In feudal times when swords were the
dominant weapon, the castle ramparts were the "high
ground." In World War II, the airplane became the
"high ground." Now, the "high ground" has shifted
to space. This upward mobility of the "high ground"
tends to be an evolutionary process. For example,
the airplane in World War I was an extension of the
ground forces used mainly for improved surveillance,
but slowly evolved to being a mobile artillery
piece. During World War II the airplane came into
its own, ranging far and wide as a strategic attack
force as well as providing cover for ground and na-
val forces. The airplane provided a means of
destroying the war manufacturing capability of an
enemy without occupying the immediate territory.
Air power starting as an evolutionary force, added a
new dimension to attack applications, and later pro-
vided a revolutionary addition to defense tactics.

Today, space is in an evolutionary phase, but by
the end of this decade it will become the "high
ground" for defense. Currently, space is being used
as an extension of our terrestrial forces, providing

improved communications, navigation, and surveillance. This function is being performed as an extension of existing systems. The Space Shuttle and new technologies now emerging will soon provide a new force and defense capability that will be revolutionary. This move to space can provide the ability to observe any location on the earth, defeat enemy long range missiles, defend space facilities, and provide instantaneous world-wide communications, command, and control. We may see space become a unified command with the elements organized much like a carrier task force, air wing, or army division (Fig. 1). In this Space Command structure large radars, optical and laser surveillance devices will be used to observe all locales on the earth's surface no matter the weather and to even penetrate the oceans. No large-scale military maneuvers will be possible without being observed. Communications will be instantaneous on a world-wide basis. Using space, we will be able to support or to provide satellite defense, destruction of enemy satellites, and destruction of enemy missiles. The possibilities also exist that we may even attack targets within the atmosphere, such as bombers or cruise missiles. These elements may all be unified by command centers located in space.

The USSR has already implemented many of the elements of a future space force including a continuously manned and resupplied space station. They have very active programs in space and a demonstrated anti-satellite capability. Table I lists their military payloads through 1975, while Fig. 2 shows the number of successful launches with no indication of a slackened pace since then. Examination of Table I shows a significant surveillance effort. "Military Recoverable Observation" was used extensively by the Soviets during the 1973 Yom Kippur War where Kosmos 596, 597, 598, 599, 600, 602, and 603 were used to monitor the battles below. Other Kosmos were used to monitor the cease-fire agreement compliance.

In order for the US to accomplish its revolutionary move to space, large and varied power systems will be required. Satellites, including the power systems, will need to be hardened and made survivable against enemy attack. Surveillance, navigation, and communication devices will require a few kilowatts up to perhaps one hundred kilowatts operating over a 5-10 year period. Solar arrays with batteries will continue to be a prime power source. However, radioisotopes will become a major
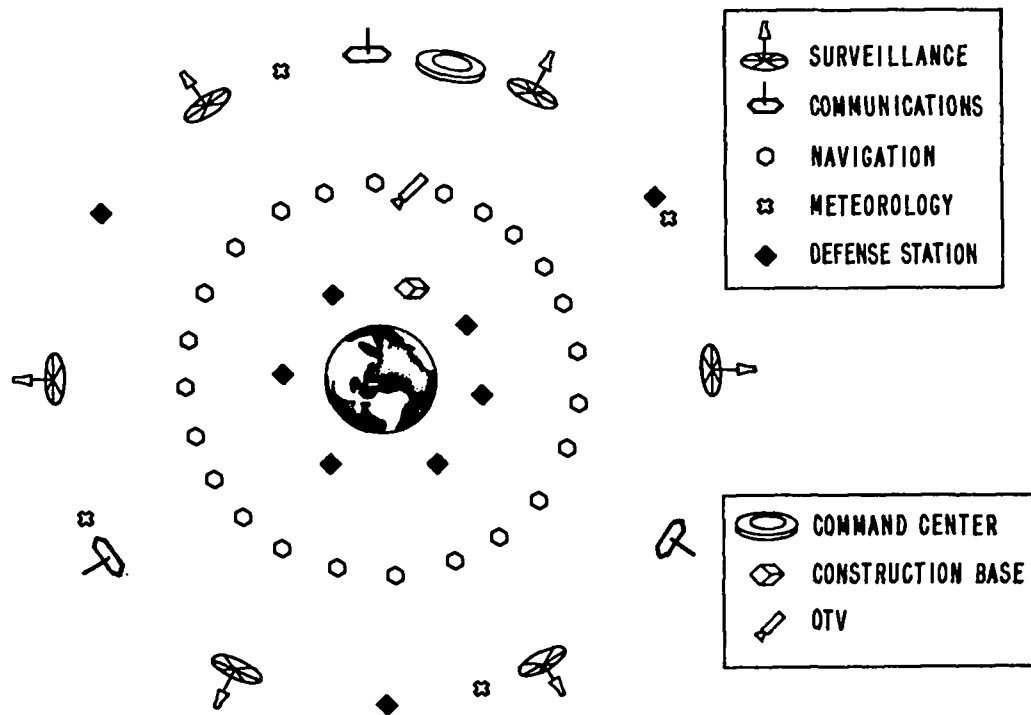

Fig. 1. Space command.

TABLE I

SUCCESSFUL MILITARY PAYLOADS

TOTALS 1957-1975 FOR U.S.S.R-U.S.*

MILITARY PAYLOAD	U.S.S.R.	U.S.
Military recoverable observation	328	220
Minor military (environmental monitoring, radar calibration, electronic ferret)	94	90
ELINT, FERRET (Satellite picks up electronic signal, communications, and radar intelligence)	42	0
Navigation and Geodesy	46	31
Military communications, store-dump	128	0
Early warning satellites (senses and transmits electromagnetic signals of nuclear explosions or missile launchings)	7	33
Fractional orbit bombardment system (FOBS)	18	0
Ocean surveillance	12	0
Inspector targets	9	0
Inspector destructors (hunter-killer anti-satellite satellites	7	0
Orbital launching platforms	135	0
TOTAL	826	374

(Includes 48 DOD civilian payloads)

Source: Staff Report, Committee on Aeronautical and Spcae Sciences, United States Senate, by Charles S. Sheldon II, CRS Library of Congress.

*Both the National Security Council and the Pentagon note there is a mistake in this table, but they are unable to supply clarification.

Reference: J. C. Glenn and G. S. Robinson, Space Trek, The Endless Migration, Stackpole Books, Harrisburg, PA, 1978.

candidate at the low-power levels because of survivability considerations. At the higher-power levels, reactors become the prime candidate because of cost and survivability considerations. For space defense, large quantities of power may be needed for short periods of time (less than an hour). This could mean chemical power or electrical power with some type of storage device. Another large power need is for orbital transfer and maneuvering. Ion propulsion using electrical power in the hundred kilowatt range offers many advantages for this.

Within the Space Command context, we can examine specific elements for their power requirements. It should be remembered that all of these elements will be necessary for an integrated effective operational force -- surveillance for detection, communications for command and control, weapons to resist attackers and to destroy enemy targets, and a command center to provide the human decision-making element and tactical implementation. In some areas, nuclear electric power plants become an enabling technology while in others it offers definite benefit/cost

advantages. The current nuclear electric power plant named SPAR is aimed at providing 100 kW_e.

To define the conditions where SPAR is an enabling technology, we used the following criteria. An operational military satellite should require no more than two Space Shuttle trips. Because the three-stage chemical Inertial Upper Stage (IUS) can deliver about 3000 kg to geosynchronous orbit, this limits the total satellite weight to about 6000 kg. However, SPAR with electric propulsion can place a 10,000 kg payload in geosynchronous orbit or for two Space Shuttle trips, the limit is 20,000 kg. This means that a single SPAR power plant with electric propulsion can do what a chemical system does in three or four Shuttle trips. The other enabling criteria is the power level for high-orbital satellites. Above about 25 kW_e, advanced solar arrays with batteries require too much of the Space Shuttle bay capacity (more than the traditional 30% weight for the power supply).

Among the missions that nuclear power may be considered enabling based on these criteria are:
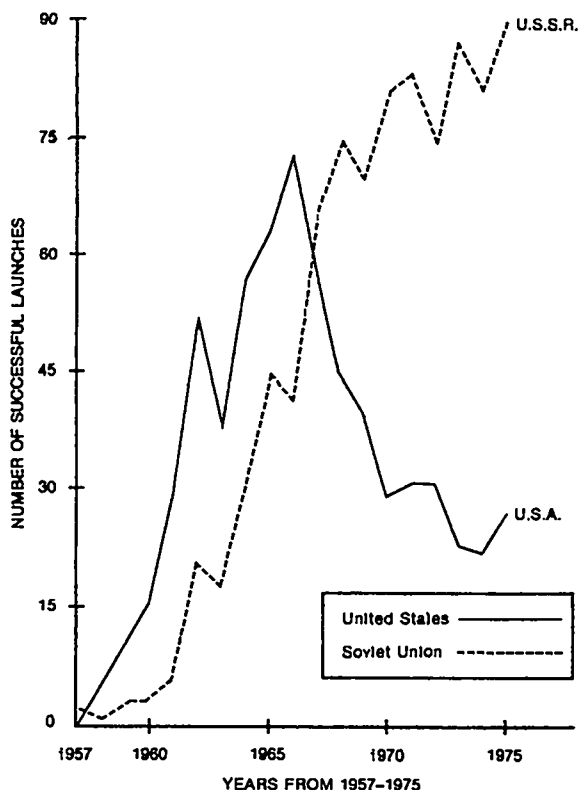
SUCCESSFUL LAUNCHES		
	U.S.	U.S.S.R.
Civil	323	292
Military	326	585

Reference: J. C. Glenn and G. S. Robinson, Space Trek, The Endless Migration, Stackpole Books, Harrisburg, PA, 1978.

Fig. 2. U.S.-Soviet record of known successful space launchings.

● Multimission space-based radar to track missiles, aircraft, and satellites;

● Multimission infrared trackers for missiles, aircraft, and satellites;

● Deep-space command center for secure and survivable command post for strategic forces;

● Tactical and strategic communications with high anti-jam capability for use with mobile terminals;

● Real-time battle communications for use by troops in the field;

● Navigation grid projection to identify locations within a battlefield;

● Control of Remote Piloted Vehicles from remote locations;

● Anti-satellite and satellite defense for maneuvering and as a possible power source for defense; and

● Real-time weather display for aircraft in flight everywhere in the world.

Besides being an enabling technology, there are some missions where SPAR offers benefit/cost advantages or other mission advantages such as survivability. These missions may be roughly characterized as high-orbital locations with spacecraft weighing between 3000-6000 kg and/or requiring 10-25 kW_e of power. These criteria were selected because they could result in the use of a single Shuttle per satellite with its resultant major reduction in transportation and assembly in space cost. Examples of these are:

● Ocean surveillance radar for tracking ships at sea; and

● Global logistics information center for world-wide inventory control.

B. Potential Peace Keeping and Arms Control Applications

One of the dominant issues in arms control agreements such as SALT is that of verification. On-site inspection has generally been deemed unacceptable. Foreign countries have proven to be uncertain locations of verification sensors such as radar, as witness Iran. Also, foreign bases have limited capability to observe certain areas within the USSR. The solution has been to locate the necessary monitoring sensors in space. However, vastly improved sensors than the current generation will be required if arms control agreements are to be more specific and applied to a greater range of armaments. For instance, if we wish to track force concentrations in a given area, vastly improved radar and optical systems are needed. These may be even larger than the multimission radars contemplated for defense purposes. The technology for such systems appears feasible and would be well worth the cost if they increase the probability of peace and security with reduced armaments. These sensors will require significant amounts of power both for propulsion to geosynchronous orbit and for operation when on station.

The use of satellites for peace keeping has already been demonstrated by the USSR to verify that the Egyptians and Israelis were adhering to the

cease fire in 1973. This type of monitoring appears to be a continuing requirement. Again, large systems in high orbits appear to offer this capability on a global basis.

C. Potential Civilian Earth-Orbit Missions

The U.S. is just beginning to exploit space, yet even these embryonic starts have greatly improved global communications, resource mapping, meteorology, and navigation. On the nightly television news, we take for granted the radar pictures from space of weather patterns and cloud cover sweeping across the U.S. Some of us remember sitting by the radio hearing the clicking of telegraph keys as we heard the World Series. Now, we watch events happening on the other side of the world as they occur, such as the Olympics. This is just the beginning. We can catch up to Dick Tracy with his wrist radio communication device. New manufacturing capabilities will exist where higher performance materials, such as magnets, ultrapure glass, and silicon are possible products.

The number of potential missions is long. Following is a list that was selected based on their potential weight, power requirements, and location in geosynchronous orbit. The work of I. Bekey, A. I. Mayer, and M. G. Wolfe[2] was used since it categorized a number of these applications by function, weight, size, power, orbit, time frame, initial operating cost, and risk. These missions include:

● Personal communications wrist telephones to serve 2.5 million people.

● Police wrist radio communications to provide real-time, secure, anti-jam, high-coverage, wide-area personal communications for policemen.

● Disaster communications to provide command and control for area emergency personnel.

● Electronic mail to transmit facsimiles of letters at reduced cost.

● National information services to provide small users rapid access to information.

● Voting or polling wrist set to provide convenient, rapid determination of the electorate's stand on candidates and issues.

● Advanced television antenna systems to provide improved television coverage, especially to mountainous, rural, and remote areas.

● Border surveillance to detect illegal aliens, drug traffickers, and others who are attempting overt or covert crossings of the border using small, sensitive, seismic sensors planted along the border and monitored from space.

● Energy monitor to fine tune energy distribution by monitoring current, voltage, or power readings on the network.

● Vehicle and package locators to be used to monitor shipments throughout the U.S. continuously and thereby minimize thefts, hijackings, and lost shipments.

● Three-dimensional holographic teleconferencing to reduce the need for travel and thereby save considerable time and money. Laser illuminators and stero sound would give the impression that all participants are present and active at the meeting.

Figure 3 shows that the above mission power requirements range from 15-220 kW_e and mass from 3000-9000 kg.

D. Solar System Exploration

Our desire to explore the universe goes beyond doing it just because it is there. An understanding of other planetary bodies leads to a much greater understanding of our own planet. Space exploration has made us realize that earth is a space-ship with limited resources and a delicate environment. With planets closer and more distant from our Sun, we can trace different stages in planetary evolution that provides clues to our own planet's past and future. Planetary exploration also provides us a chance to better understand the natural laws that govern all processes. Using the Earth as a vantage point for understanding the behavior of nature is limited by forces such as gravity and magnetisms that are associated with Earth's environment. As we reach out into space, we are able to observe phenomena not discernible within the Earth's environment that may lead to fundamental changes in our definition of the laws of physics. This better understanding might someday lead to solving everyday problems such as fusion for unlimited energy. Besides an improved knowledge of the solar system and improved understanding of scientific phenomena, planetary exploration is laying the foundation for future exploitation of space resources and possible colonization. Also, we are taking our first small steps to other stars.

Solar system exploration missions are being performed at greater distances from the earth and in

5

```
          12,000 ─

          10,000 ─
                        ELECTRONIC MAIL
                           ▲  ▲ VEHICLE/PACKAGE LOCATOR
                        NATIONAL INFO SYSTEM
       ‿                                  ▲ POLICE WRIST RADIO
       ⌒          8000 ─                  ▲ DISASTER COMMUNICATIONS
       ┐
    MASS (kg)                   ▲ WRIST COMMUNICATIONS
                        HOLOGRAPHIC TELECONFERENCING▲
                                      NATIONAL TV▲
                  6000 ─                    ▲ VOTING WRIST SET

                              ▲ ENERGY MONITOR
                  4000 ─
                            ▲ BORDER SURVEILLANCE

                  2000 ─


                       10              100             1000
                              POWER (kWₑ)
```

SOURCE ADVANCED SPACE SYSTEM CONCEPTS AND THEIR ORBITAL SUPPORT NEEDS (1980 2000)
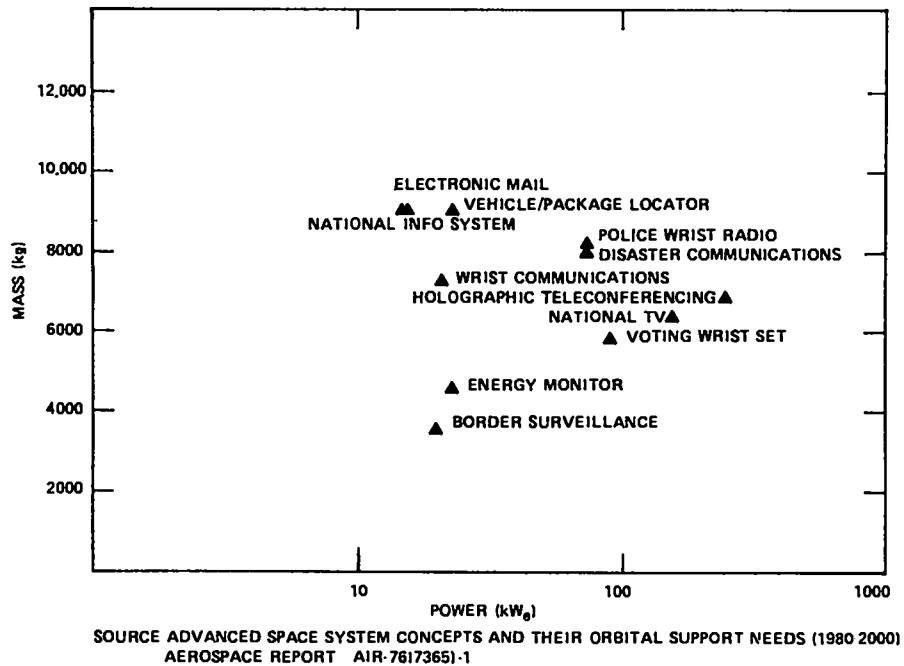AEROSPACE REPORT   AIR-7617365)-1

Fig. 3. Potential civilian applications in geosynchronous orbit.

ever increasing detail. Exploration has progressed
from reconnaissance probes of bodies in the solar
system to the exploration of these bodies with or-
biting sensors and landers followed by intensive
studies using rovers and surface sample and return
techniques, and may finally lead to establishing
semipermanent or permanent bases.

Figure 4 depicts expected growth for planetary
missions with the capability expected from various
propulsion modes.[3] Chemical power has been the
major propulsion source to date, but the limits of
its capability will be reached in missions during
the 1980s. Solar Electric Propulsion (SEP) with ion
thrusters will extend the ability to perform plane-
tary missions and meet requirements for the late
1980s and early 1990s, but its limit will be reach
in reconnaissance missions to Uranus and exploration
missions to Saturn. Nuclear Electric Propulsion
(NEP) with ion thrusters extends the capability to
investigate the outer planets and to perform solar
escape missions. The nuclear electric propulsion
power supply envisioned here uses a 400-kWₑ power
plant. A significant advantage is obvious for nu-
clear electric propulsion, especially as the dis-
tance from the Sun increases.

A 100-kWₑ power plant such as SPAR can provide
significant capability over the SEP system shown in
Fig. 4, and provide the experience and technology
base for the longer duration, more distant missions
to Pluto and beyond. For instance, based on recent
studies at the Jet Propulsion Laboratory, the pay-
load to the Asteroids is tripled using SPAR as a
power source for electric propulsion and reconnais-
sance missions to Uranus and Neptune become feas-
ible. Nuclear power is an enabling technology if we
are to pursue our planetary program to the outer
planets.

E. Transportation to Geosychronous Orbit

A number of candidate systems exist to move
satellites from low to geosynchronous orbit. Some
of these are one-time-only systems and others are
based on reusable vehicles. The characteristics of
the transfer will determine the type of propulsion
desirable. Chemical systems tend to perform the
transfer in a matter of hours at high acceleration
levels. Electrical propulsion with ion thrusters
take hundreds of days to perform a similar trans-
fer. However, the stage weights are considerably
less with ion thrusters. Chemical rockets can be
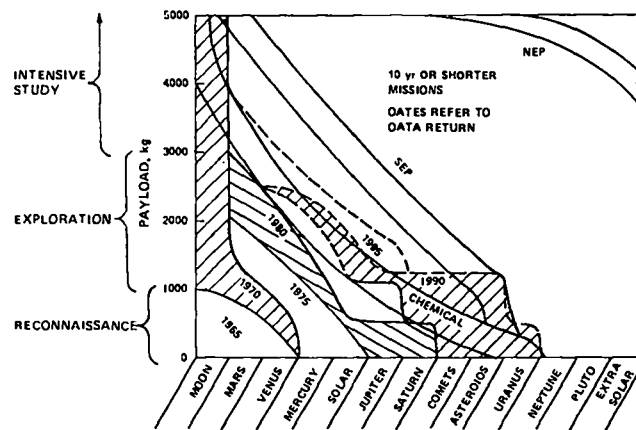characterized as high thrust but limited specific

Fig. 4. Solar system exploration.

impulse systems, while electrical propulsion are limited thrust but high specific impulse systems. A number of potential orbital transfer vehicles are compared in Fig. 5.

The Inertial Upper Stage (IUS) that is currently being developed as a standard module for the STS consists of a two-stage vehicle 4.5 m in length. It is capable of transporting a payload of 2270 kg to geosynchronous orbit. There is also a three-stage version that is formed by adding another large motor as a lower stage to the two-stage vehicle. It is 6.4 m in length and can deliver 3180 kg to geosynchronous orbit.

Transtage, Agena, and Centaur, current upper stage chemical rockets, provide limited payloads to geosynchronous orbit. A number of advanced chemical stages, Low Thrust Liquid (LTL), All Propulsion Orbit Transfer Vehicle (APOTV), and Aeromaneuvering Orbit Transfer Vehicle (AMOTV) are being investigated. The LTL can deliver twice the payload to geosynchronous orbit as a three-stage IUS. Also shown in Fig. 5 is the nuclear electric propulsion stage (NEPS) using a 100-kW$_e$ power plant. The delivery capacity is three times that of the three-stage IUS. NEPS can deliver large payloads compared to chemical stages, but at a cost in delivery time (150-225 days compared to one day or less).

If solar arrays are incorporated into the spacecraft, then these can be used as a power source for ion thrusters. Because of higher mass and large volume, solar arrays can deliver about half the mass and require twice the time compared to nuclear electric propulsion. One reason for their poorer

performance is that about one-third of the solar array power is lost from degradation in the Van Allen belts.

Nuclear power appears to offer an interesting option for one-way transfer of spacecraft to geosynchronous orbit or possibly as a space tug (depending on safety aspects) where transfer times of a half year are acceptable. The larger payload capability compared to either chemical stages or solar arrays and the ability to endure long time periods in the Van Allen belts are definite advantages. In addition, experience will be gained for planetary missions in the 1990s.

F. Power Plant Requirements

1. POWER OUTPUT. Nuclear power requirements in geosynchronous orbit cover the range from 10-100 kW$_e$ for potential defense missions and 15-220 kW$_e$ for potential civilian applications. For planetary missions, 400 kW$_e$ appears desirable.

2. LIFETIMES. Lifetimes are established by anticipated development of other components in the spacecraft. Goals of 7-10 years have been established for spacecraft in geosynchronous orbit and 10 years for planetary missions.

3. RELIABILITY. Power subassembly reliability of 0.95 is the design goal for geosynchronous orbit and as high as possible for planetary missions. Designs that avoid single-point failures and degrade gradually are favored.

4. MASS. A general rule of thumb is that the power subassembly will require up to 30% of total space mass. For a dual Shuttle-launch spacecraft, the goal is 1910 kg.
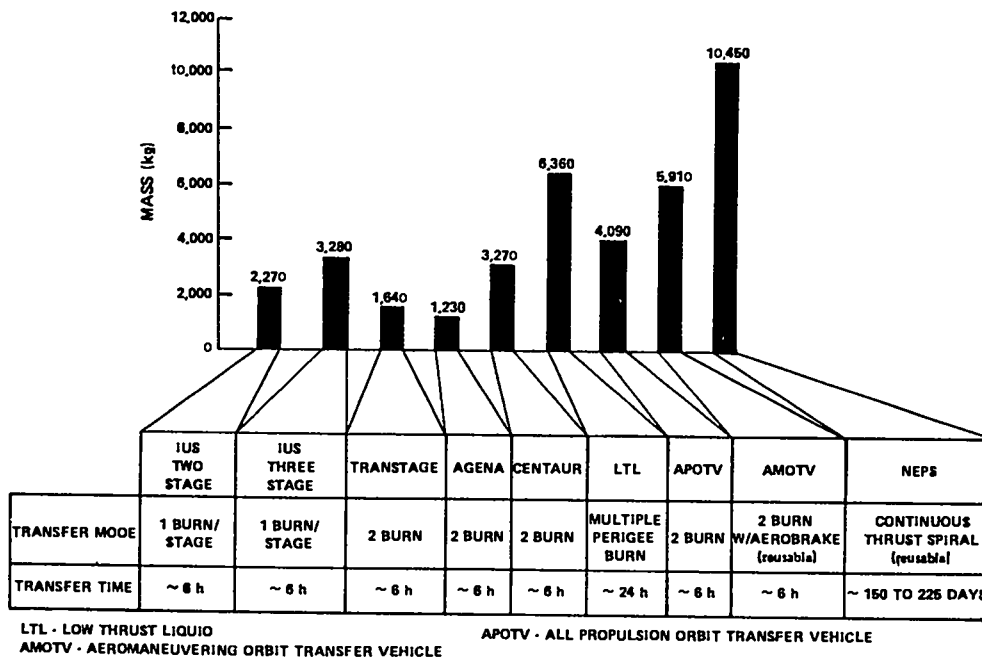
7

Fig. 5. Orbit transfer system performance comparison (low earth orbit to geosynchronous orbit).

MASS (kg)

Bar values: 2,270 · 3,280 · 1,640 · 1,230 · 3,270 · 6,360 · 4,090 · 5,910 · 10,450

	IUS TWO STAGE	IUS THREE STAGE	TRANSTAGE	AGENA	CENTAUR	LTL	APOTV	AMOTV	NEPS
TRANSFER MODE	1 BURN/STAGE	1 BURN/STAGE	2 BURN	2 BURN	2 BURN	MULTIPLE PERIGEE BURN	2 BURN	2 BURN W/AEROBRAKE (reusable)	CONTINUOUS THRUST SPIRAL (reusable)
TRANSFER TIME	~6 h	~6 h	~6 h	~6 h	~6 h	~24 h	~6 h	~6 h	~150 TO 225 DAYS

LTL · LOW THRUST LIQUID
AMOTV · AEROMANEUVERING ORBIT TRANSFER VEHICLE
APOTV · ALL PROPULSION ORBIT TRANSFER VEHICLE

5. CONFIGURATION CONSTRAINTS. The Space Shuttle dimensions of 18.3 m length and 4.5 m diameter limit the volume allowable for the power source. The individual spacecraft will determine how much volume can actually be used by the power source.

6. RADIATION. The spacecraft must be able to operate in natural radiation fields. Induced radiation created by nuclear power systems must be reduced to an acceptable radiation level determined by spacecraft components. For present electronic components, it is 10^{13} nvt and 10^7 rad over the mission life.

7. SAFETY FEATURES. The power subassembly must meet all regulations of NASA, DoD, DOE, and the National Range Commmanders. All payloads using the STS are subject to a uniform set of basic safety and interface verification requirements. The safety requirements are tailored to identify the hazard potential of the payload. The Payload Safety Guidelines Handbook (JSC-11123) provides a basis for selecting design options to eliminate hazards. The STS safety policy requires that the basic payload design assure the elimination or control of any hazard to the Orbiter, crew, or other payloads.

Table II provides a summary of power plant requirements.

II. POWER PLANT DESCRIPTION[4]

A. General Configuration

An extensive review of design alternatives for a nuclear reactor space power system capable of delivering 10-100 kW_e has led to the selection of a heat-pipe-cooled fast spectrum reactor with a thermoelectric power conversion system. The general features of this system are illustrated in Fig. 6. The reactor design features a beryllium reflector, laminated core configuration with sheets of molybdenum extending across the full diameter of the core and interspersed between layers of UO_2. Reactor heat is transferred by the sheets from the UO_2 to an array of some 90 Mo/Na heat pipes. The heat is then transported by the heat pipes around the LiH shield to a ring of high-power density thermoelectric modules constructed from modified SiGe alloys. Conversion takes place over a temperature interval of 1375-775 K with an efficiency of 9%. Residual heat is rejected by a radiator that is constructed using heat pipes.

Avoidance of single point failures and propagating failure chains has constituted the main design emphasis for the SPAR system. Currently, no single failure points are known to exist in the power

TABLE II
POWER PLANT REQUIREMENTS

	Requirement	
	Geosynchronous	Planetary
Power output (kW$_e$)	10-100*	400
Lifetimes (y)	7	10
Reliability	0.95	High as possible; no single point failures
Mass (kg)	1910	8000 (includes power conditioning and larger shield)
Configuration constraints	Minimize packaging volume in shuttle bay	Minimize packaging volume in shuttle bay
Radiation attenuation		
Neutrons (nvt)	10^{13}	10^{12}
Gamma (rad)	10^7	10^6
Maneuverability	Mission dependent	Ion thrusters
Safety	STS requirements	STS requirements

*NASA requirements could extend this to 220 kW$_e$.

plant. Thus, the core contains 90 separate thermally-coupled heat transfer loops, each with an associated power conversion module. Connecting modules in a series-parallel network makes it possible to tolerate the loss of several of these units while still maintaining operational capability for the system as a whole. Interconnecting the heat pipes in the waste heat removal system yields a network that is highly tolerant of heat pipe failures.

B. Reactor Design and Shield

Early designs of the SPAR core featured hexagonal fuel elements of molybdenum-encased UC-ZrC, each of which was cooled by a separate heat pipe constructed of molybdenum with sodium working fluid. Interelement heat transfer, required to accommodate potential core heat pipe failures, was to be achieved by a core banding system that established thermal contact by compressing deformable

Fig. 6. Layout of SPAR power plant.

foil placed between fuel elements. This system had a number of design uncertainties that would have required extensive development and testing to resolve. It was also difficult to power flatten, partly due to its basic hexagonal geometry. However, it was not these considerations but rather the desire to avoid the development and fabrication problems anticipated for the carbide fuel that set in motion the innovation chain leading to the present design. Specifically, it was the desire to build a UO_2-fueled core without sustaining too large a reactor size and weight penalty that led to a layered Mo-UO_2 fuel configuration that was eventually expanded from a single fuel element to the current integral core design.

The integral core SPAR design is shown in Fig. 7. The core is contained within a cylindrical molybdenum can having a diameter of 290 mm and a height of 290 mm. Because the can is not designed as a pressure vessel, its walls and one end plate are only 2 mm thick. The other end plate, which serves as the mounting plane for the heat pipes, is 6 mm thick. Within this can are 90 molybdenum heat pipes encased in a fuel that consists of alternate layers of UO_2 and molybdenum. The core is reflected radially and on one end by beryllium. The other end reflector is BeO that is mounted around the heat pipes within the molybdenum core container. Control of the reactor is provided by twelve rotating beryllium drums each with B_4C segments mounted on one side. Key design parameters of the reactor are given in Table III.

The interleaving of sheets of molybdenum between layers of UO_2 has provided a fuel form that has
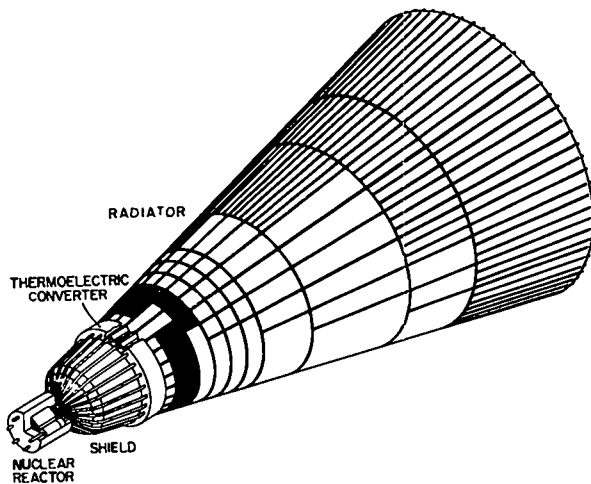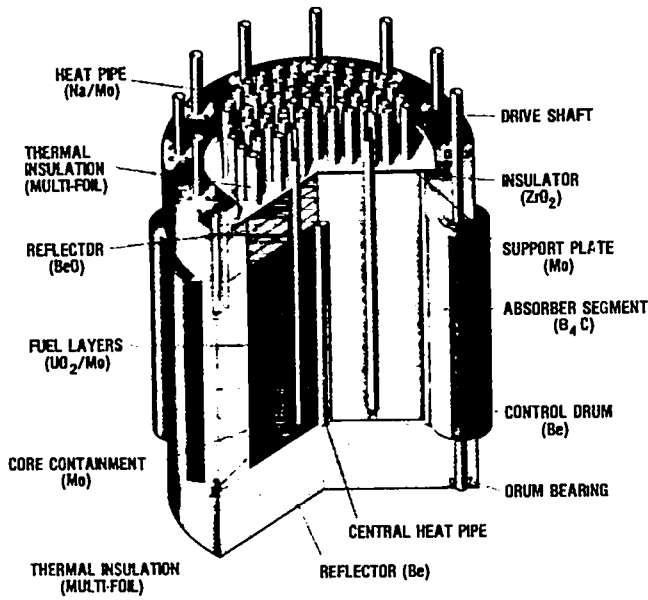
9

Fig. 7. Cutaway view of SPAR assembly.

made possible a relatively compact UO_2-fueled core
with a number of design simplifications over previ-
ous SPAR configurations. Compactness results from
the high volume fraction of UO_2 in the fuel. This
could be done without causing excessive fuel temper-,
atures because the layered configuration maximizes
the thermal conductivity of the fuel for a given
amount of added molybdenum.

Figure 8 shows one method by which the layered
fuel can be attached to heat pipes. Heat generated
in the UO_2 is conducted to the molybdenum sheets
and thence along these sheets to the heat pipes,

where thermal contact is made by a spring tab con-
figuration. Each sheet is in thermal contact with
the entire complement of core heat pipes. The core
is built up by pressing one sheet at a time over the
heat pipe array, which is held firmly in place by
the molybdenum end plate. The UO_2 is in the form
of tiles, shaped as shown in Fig. 8. A complete
layer of these tiles can be attached to each molyb-
denum sheet with a vaporizable bonding agent to
simplify assembly.

One of the important design simplifications that
has been made possible by the layered fuel configur-
ation is that the core is cylindrical. This not
only reduces critical mass because of reduced neu-
tron leakage, but also eases the assembly procedure
and makes the reflector design more tractable. The
layered fuel adds confidence to the ability of the
system to withstand heat pipe failures because it
removes the concern with thermal bonding between
fuel elements. It markedly improves the tolerance
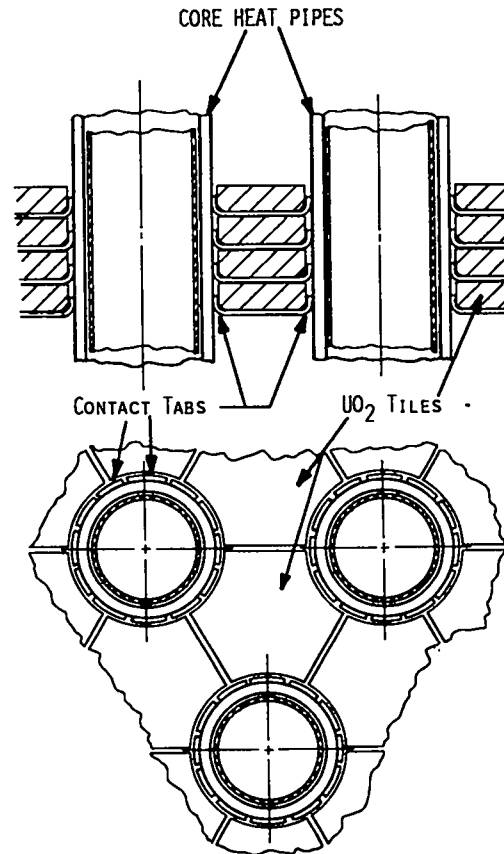of the system to failure of heat pipes on the core

TABLE III

SPAR DESIGN PARAMETERS

Reactor Power (kW$_t$)		1100
Core diameter (mm)		290
Core height (mm)		290
Number of core heat pipes		90
Core heat pipe temperature (K)		1400
Reactor diameter (mm)		520
Reactor height (mm)		500
Reactor mass (kg)		400
Fuel region	125	
Reflector	160	
Heat pipes	55	
Control system	35	
Support structure	25	

Fig. 8. Layered Mo-UO_2 fuel arrangement.

periphery because the outer molybdenum can is able to serve as an additional thermal conduction path for removing heat from the fuel surrounding an inoperable heat pipe and transporting it to neighboring heat pipes.

Perhaps the most important design simplification made feasible by the layered fuel concept is the ease with which radial power flattening can be achieved. This can now be done by arranging the heat pipes in concentric rings and varying the spacing between heat pipes from one ring to the next so that the total heat flux transmitted to each heat pipe is constant. This is accomplished with no variation in fuel enrichment. Hence, no significant increase in core size and mass is needed to produce a power-flattened core.

Still another simplification feature attributable to the layered fuel configuration is the manner in which fuel swelling can be accommodated. Room for radial fuel swelling can be obtained by allowing space between UO_2 tiles. Space for axial swelling is easily introduced, where necessary, by periodically leaving unfilled space between the molybdenum sheets when the stack is assembled.

Shield design and technology make extensive use of work on space reactor shields for SNAP 2, 8, and 10A, and of ROVER experience. These reactors have certain features in common with current designs, namely, small physical size, unmanned space application with comparable allowance for neutron and gamma doses, and comparable radiation flux levels.

Only shadow shielding is required because:

● Only unmanned power plant operation is considered.

● The reactor will be used only in high-Earth orbit, where neutron and gamma scattering from air is negligible.

● The reactor can be located at one end of the assembly, followed by the shield, control actuators and radiator, and, finally, the payload.

The shield can be considered as follows: Neutron attenuation is provided by lithium hydride (LiH) in the shape of a frustum, and a heavy-metal gamma shield is added at the reactor end of the shield if needed.

Lithium hydride dissociates unless an overpressure of hydrogen is provided. Also, the LiH is maintained at a minimum temperature of 600 K during operation so radiolytically decomposed hydrogen will be reabsorbed by the LiH and prevent swelling.

To minimize single-point failures, the LiH is to be encapsulated in a number of pancake-shaped cans so that pressure containment failure from meteoroid penetration or a weld failure, for example, will deplete the hydrogen in only a small part of the shield. The shield is also a structural member that connects to the reactor on one end and by a boom to the payload on the other.

C. Conversion System and Radiator

Power conversion for the SPAR system is accomplished by a network of thermoelectric elements based on silicon-germanium alloys. These elements are built into cylindrical modules surrounding the core heat pipes as shown in Fig. 9. In this unit, six n-p couples are positioned circumferentially around the core heat pipe in a series configuration that yields approximately 1 volt output under normal operating conditions. The module is formed by placing these ring units adjacent to each other along the pipe, the number being determined by the output voltage desired. For power levels of 100 kW_e, a voltage level of 100-150 Vdc is desirable in order to minimize the power transmission line weights.

Not shown in Fig. 9 is the system to remove reject heat from the outer periphery of the module. This can be done either by a single annular heat pipe enclosing the entire module or by a redundant system of small annular heat pipes about each of the thermoelectric ring units. The latter configuration is illustrated in Fig. 10. The coupling heat pipes
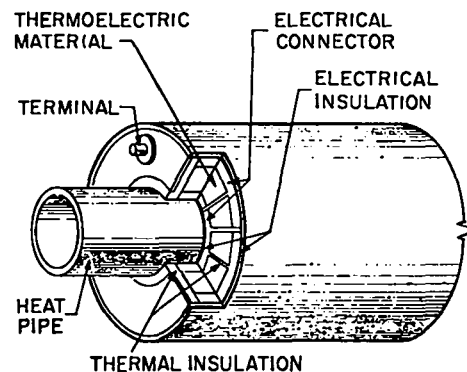

Fig. 9. High power density thermoelectric module.

11

serve to change the geometry from cylindrical to square in order to achieve good thermal contact with the radiator stringer pipes. The latter are shown with a rectangular cross section at the evaporator end and are arranged so that several cool each thermoelectric module.

As Fig. 10 illustrates, five thermoelectric modules are grouped together to form a basic panel segment of the thermoelectric conversion and radiator subsystems. The coupling heat pipes of adjacent thermoelectric modules are thermally connected so that if one of the radiator stringer heat pipes should fail, its heat load is shared by nearby stringers.

The stringer heat pipes are made of titanium because of its relatively low density combined with high temperature capability. Current designs are stressing minimal heat-pipe wall thickness and the potential use of lightweight armor layers such as carbon, silicon, aluminum, or refractory compounds on the side of the stringer exposed to meteoroid flux.

The manner in which the radiator panels are displayed to form the full radiator is illustrated by Fig. 11. With a total of eighteen segments, the array is approximately cylindrical with a diameter that just fits into the bay of the shuttle launch vehicle. The cylindrical configuration is favored because packaging considerations in the shuttle bay may rival power plant mass in importance. The radiator is a dominant length element and can be packaged in a number of configurations (Fig. 12). The cylindrical arrangement is very convenient because it allows storage inside the radiator during shuttle
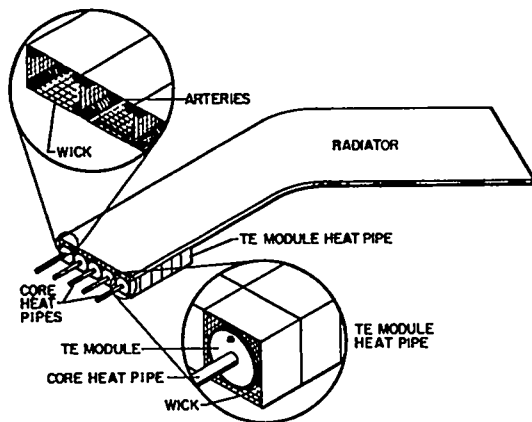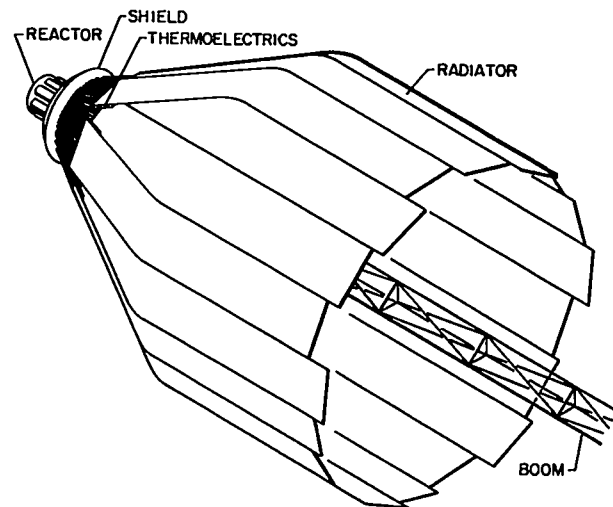

Fig. 11. Space nuclear power plant.

flight. Figure 13 shows a structure stored inside the radiator in stowed and partially deployed configurations.

D. Operating Parameters for 10-100 kW$_e$ Power Plants

Table IV gives operating parameters for the SPAR system at various design powers. The thermoelectric module efficiency is taken to be 9%. This value is based on work done on SiGe alloys modified with GaP additive to decrease thermal conductivity.

E. Power Plant for 400 kW$_e$

Design studies of a nuclear reactor to provide thermal power to an electric propulsion system for deep space exploration have been ongoing for several years. The present design goals are to produce 3 MW$_T$ of power for 75,000 full-power hours during a mission lifetime of 12 years to drive a thermionic electrical conversion system operating at a source temperature of 1650 K.

The reactor design has evolved to a configuration very similar to the one for 1.2 MW$_t$. However, it contains 162 heat pipes. The heat pipes are still molybdenum but, because of the higher temperature, they use lithium as the working fluid. Figure 14 is a layout of the core. The reflector is all BeO because of the higher operating temperature, and the number of control drums is increased to 16 because of the larger core diameter.

The reactor design is described in Tables V-VII. Fuel swelling for the layered integral core design was estimated from BMI data[5] for pure UO$_2$, which
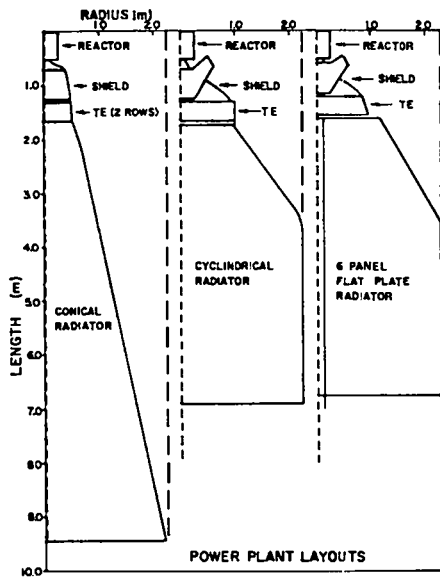

Fig. 10. Radiator segments.
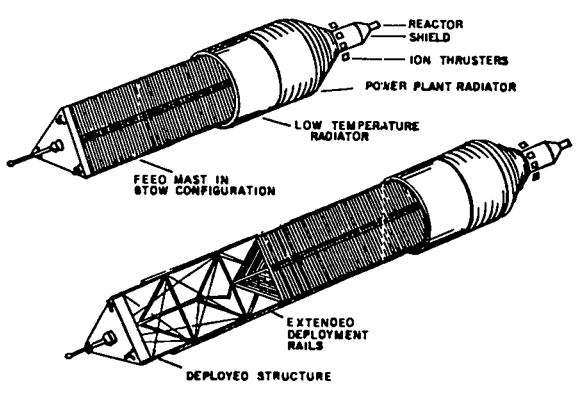
Fig. 12. Power plant layouts.

Fig. 13. Nuclear OTV stage.

has a considerably higher swelling rate than UO_2 in a molybdenum matrix. It is not clear that the BMI data is directly applicable to the layered core concept because the temperature gradient in the UO_2 will be much smaller in the reactor than it was in the BMI experiments. As a consequence, it is possible that swelling extrapolated from this data is overestimated. In any case, the required void allowance for fuel swelling can easily be incorporated in the layered core design simply by including gaps between layers in the core, and between the UO_2 tiles.
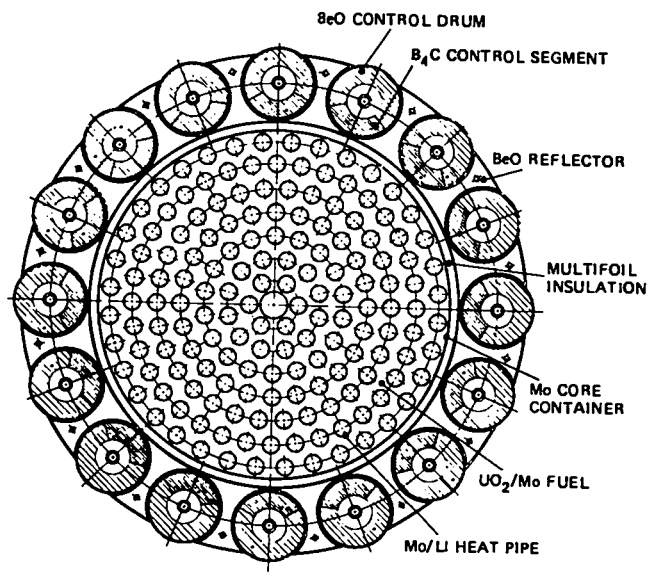

Fig. 14. Cross section of a 3-MW layered integral core reactor.

TABLE IV

OPERATING PARAMETERS OF SPAR THERMOELECTRIC

POWER PLANT (7 yr Lifetime)

		Power (kW$_e$)	
	10	50	100
Reactor power (kW$_e$)	110	550	1110
Core heat pipe temperature (K)	1400	1400	1400
Fuel swelling (%)	1	2	3
Burnup fraction - ^{235}U (%)	1	2	4
Thermoelectric efficiency (%)	9	9	9
Radiator temperature (K)	775	775	775
Radiator power (kW$_t$)	100	500	1010
Power plant mass (kg)	810	1255	1775
Reactor	400	400	400
Shield	255	335	380
Thermoelectric converter	30	140	285
Radiator	50	255	530
Structure	75	115	160

13

TABLE V
REACTOR DIMENSIONS

	Laminated Core
Core diameter (mm)	390
Reactor diameter (mm)	620
Core length (mm)	390
Reactor length (mm)	600
Reflector thickness (mm)	100
Number of heat pipes	162
Average heat pipe spacing (mm)	29.1
Heat pipe outer diameter (mm)	20.0
Heat pipe vapor area (mm^2)	188
Fuel vol. fraction (assuming 100% dense)	0.461*

*80 vol% UO_2-20 vol% Mo fuel

TABLE VI
REACTOR WEIGHT SUMMARY (kg)

		Laminated Core
Mo-UO_2 fuel, total weight		231
UO_2 only	187	
^{235}U only	154	
Mo heat pipes, 110 kg/m		
(to outer edge of reactor only)		54
BeO reflector		342
Control system		75
Reactor support structure		35
TOTAL		737

TABLE VII
REACTOR OPERATING CHARACTERISTICS

	Laminated Core
Nominal electrical power output (kW$_e$)	400
Thermal power level (MW$_{th}$)	3
Thermionic converter efficiency (%)	15
Lifetime at full power (h)	75000
Number of heat pipes	162
Nominal UO_2 content of fuel (vol %)	80
Average power density in Mo-UO_2, (MW/m^3 or W/cm^3)	114
Average power density in UO_2, (MW/m^3 or W/cm^3)	143
Power per heat pipe (kW)	18.8
Heat pipe axial heat flux (MW/m^2)	100
Heat pipe radial heat flux (MW/m^2)	1.00
Heat pipe temperature (K)	1675
Average fuel temperature (K)	1763
Maximum fuel ΔT (K)*	199
Maximum fuel temperature, (K)*	1906
^{235}U burn up (%)	7.1
Fission density in Mo-UO_2 (10^{20} fissions/cm^3)	9.2
Fuel volume swelling (%)	20
Reactivity change Δk due to fuel burn up (%)	4.3
Reactivity change Δk due to thermal expansion (%)	2.1

*Assumes a 1.5 peak-to-average power density ratio.

III. SAFETY ASPECTS OF A NUCLEAR POWER SOURCE

The US position concerning safety of nuclear reactors in space is summarized in the following excerpts from a working paper submitted to the United Nations Committee on the Peaceful Uses of Outer Space, Scientific and Technical Sub-Committee, in February 1979.

"U.S. safety philosophy relative to space reactors has not been re-examined since the development and launch of the SNAP 10A SNAPSHOT. However, the basic design philosophy developed for that launch is, in principle, still valid." ...The basic safety requirement is no undue risk to the public or the environment. In the case of nuclear reactors which have operated, the primary concerns are the release of fission products from the reactor core and high-level external radiation from an intact core or from activated components of the reactor's structure. These concerns can be minimized or eliminated by restricting the use of the reactor to high earth orbit. Hence, a basic criterion for space reactor operation could be to launch unoperated reactors which are started after a safe altitude is confirmed. The U.S. currently defines a safe altitude as one where the lifetime is greater than 300 years (400 nautical mile circular orbit). This would allow sufficient time for the fission products and activated materials to decay to safe limits before re-entry. Another consideration would require controls to prevent inadvertent criticality of the reactor in the event of launch accidents."

The key to safe operation before and during launch is to keep the reactor in a nonoperative mode. This is accomplished by adding built-in safety features, such as redundant control elements, where only one element is allowed to be unlocked at a time; brakes on the control element actuating mechanisms to prevent movement without two independent signals; and a reactor designed to remain nonoperative even with environment changes, such as immersion in water. Before operation, the reactor and its uranium fuel are perfectly safe to handle. There is no possibility that a nuclear explosion can result from a space reactor power plant.

Analyses and tests are used to demonstrate safety aspects in case of launch pad fires, propellant fire, impact at terminal velocity in case of a launch abort or failure to reach orbit, and water impact. Again, the major requirement for safety is not to operate the reactor until the prescribed orbit is reached.

Most applications considered for nuclear reactors are in high orbits, such as geosynchronous. The higher the orbit, the longer a satellite will remain in orbit. Long orbit times provide time for radioactive elements to decay. An orbit altitude of 400-500 n mi will provide for over a 1000-yr life and thus could give a margin of conservatism in meeting safety criteria. Doubling the orbit increases the orbital lifetime to about a million years. Satellites in geosynchronous orbit (19 400 nautical miles), the proposed location of most reactor-powered US satellites, will, for all practical purposes, never re-enter the Earth's atmosphere.

The only US reactor flown in space, SNAP 10A in 1965, was not operated until its 700-n mi orbit was achieved. SNAP 10A's estimated orbital lifetime is 3800 yr.

Current US design philosophy is to have the reactor disintegrate and the core disperse on re-entry into the atmosphere. This can be accomplished by atmospheric heating, chemical reactions with the atmosphere, and physical forces imposed by the reentry into the atmosphere. The reflector could act as a heat shield on re-entry and, hence, it will be necessary to design it to separate in the upper atmosphere. Though the details of space nuclear power system designs are under development, we anticipate that the reflector will be held together by bands that will melt on reentry as a result of atmospheric heating. The molybdenum heat pipes and structure in the core will oxidize, allowing the fuel to disperse into the atmosphere. The radiation level of any element or particles reaching the Earth's surface will be extremely low after the long orbital times provided for radioactivity decay and will not pose a health hazard.

Since nuclear safety is based on the principle of in-depth defense against possible miscalculations, an anlysis has been performed on the effect of the reactor re-entering intact after low-altitude orbit operation followed by a failure of the nuclear electric propulsion stage. This should be the most serious health hazard to the general population. Even under these circumstances, the radiation levels can still be low enough to not present a health hazard. Figure 15 shows gamma activity as a function of run time for an intact reactor. This information
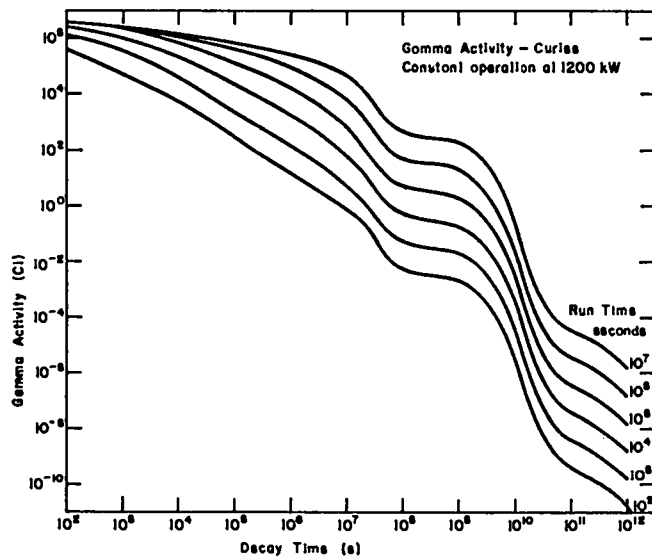
Fig. 15. Gamma activity as a function of time.

was combined with orbital lifetimes before re-entry for different initial starting altitudes and for different power plant operating times prior to a terminating operation. The initial orbits were based on the number of Orbital Maneuvering Subsystems (OMS) employed with the STS. Figure 16 is constructed on the assumption that the reactor will be operated the equivalent of one-hour full power prior to activation of the ion thrusters to checkout the power system. Then, the altitude was computed for 1 hr, 1 day, 1 week, and 1 month of operation and an orbital lifetime determined assuming a spacecraft failure at these points in time. Using Fig. 15, the gamma activity was determined at the time of re-entry and this information is plotted in Fig. 16. The safety region in Fig. 16 represents approximately a 300 yr orbit time. The following conclusions, based on the assumption that somehow the power plant would reach the Earth's surface intact, are reached after examining the figure.

- If two OMS kits are used so that the initial orbit is 850 km (460 n mi), regardless of the time that a failure occurs after initiating reactor operation, there would be no risk to the general population;

- If one OMS kit is used so that the initial orbit is 620 km (335 n mi), the possible risk period is a few days;

- If no OMS kits are used starting at an altitude of 450 km (240 n mi), the possible risk period is about a week.

It is concluded that orbital transfer with a nuclear space power system can be made very safe from a low orbit and as higher altitudes are achieved by the nuclear propulsion transfer vehicle, the system becomes increasingly safe.

IV. PROGRAM PLAN FOR 10-100 kW$_e$ POWER PLANT

A technology readiness program has been initiated to demonstrate that key components of the reactor/thermoelectric power system can be constructed to meet performance objectives for the required 7-10 yr lifetime. The goal of this program is to bring the power plant technology to the point where the technical risk involved in undertaking the building and testing of a groundbased prototype of the system is low. The general types of information needed to reduce this risk include: understanding the basic physics; knowledge of basic material properties; demonstration of our ability to fabricate the components of the power plant; demonstration that these components will behave as specified; understanding of power plant assembly; and demonstration of our ability to meet safety requirements.

The basic physics of the power plant and its components is straightforward for today's
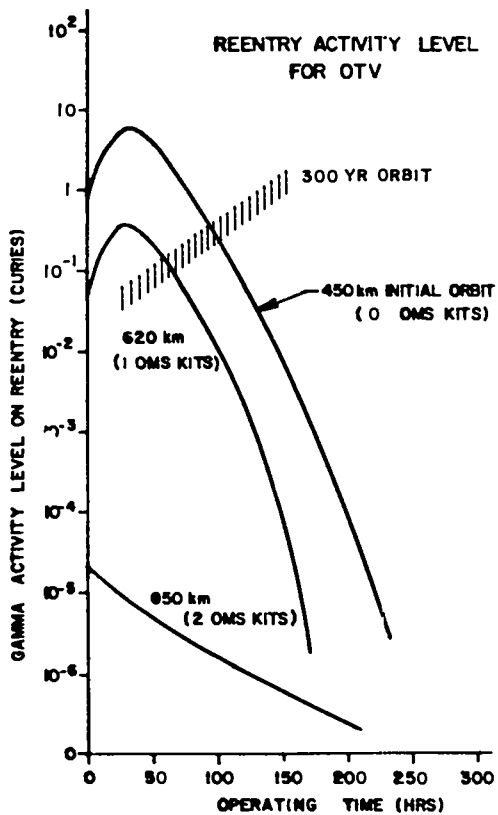
**REENTRY ACTIVITY LEVEL
FOR OTV**

300 YR ORBIT

450 km INITIAL ORBIT
(0 OMS KITS)

620 km
(1 OMS KITS)

850 km
(2 OMS KITS)

Fig. 16. Reentry activity level for OTV.

technology. Reactor neutronic and kinetic calcula-
tions, radiation shielding, converter technology,
and radiator technology are all well established.
The state of understanding of the properties of the
materials used in the SPAR system is not quite so
complete. In general, sufficient data exists to
give high confidence in the technical feasibility of
the SPAR design, but in some instances extrapolation
of known data to the 7-10 yr lifetime of SPAR en-
genders uncertainties that have been compensated by
increasing system weight.

Some of the design innovations of the SPAR
system call for fabrication procedures that have not
been specifically applied to the SPAR components. A
major part of the technology readiness program is to
adapt these procedures to SPAR component production
and show, through accelerated testing in simulated
launch and space environments, that the resulting
components meet the reliability and lifetime
requirements. An extension of this activity is the
assembly of portions of the power plant to ensure
that interactions between sections of the complete

thermal and electrical systems are well understood.
Such tests will serve to verify the conclusion of
the extensive system design and analysis effort that
provides the guideline for the technology readiness
program.

Overlying the system design and analysis effort
and technology readiness program is the considera-
tion of system safety. The determination of what
constitutes safe launch procedures and safe opera-
tion in orbit is not static and modification in
reactor design as well as tests in addition to the
currently planned water immersion criticality meas-
urements and propellant fire effects must be
expected.

The technology readiness program has been in-
dexed in terms of the following system components:

1. Nuclear reactor plus heat pipe system for
   transferring heat to converter.
2. Radiation shield for protection of payload
   components from neutron and gamma radiation.
3. Thermoelectric conversion system.
4. Radiator heat rejection system.

The program for developing the reactor technol-
ogy includes comprehensive engineering design and
analysis of the core, reflector and control system
with heavy emphasis on the ability to withstand the
launch environment, and on safety.

A series of critical assemblies will be con-
structed, primarily to establish firm data for reac-
tor control and safety analysis. Performance con-
firmation and reliability testing will be done for
the molybdenum core heat pipes and for the fuel/heat
pipe combination. The latter testing will include
irradiation testing in the EBR-II reactor.

Mechanical actuators for SNAP have been individ-
ually tested for over three years. However, the
effect of going from three year to seven year per-
iods on the durability of mechanical devices is hard
to project. A thorough examination of previous ac-
tuator performance data and accelerated testing of
actuators will be used to verify technical readiness.

Shield design will rely heavily on Monte Carlo
analysis and on work done as part of the nuclear
rocket and SNAP space reactor programs. The planned
canning of the LiH shielding material in a large
number of separate stainless steel containers pro-
vides the redundancy needed to offset potential con-
sequences of the appreciable hydrogen overpressure

of this material at temperature on the order of 700-800 K.

The thermoelectric conversion units are based on SiGe alloys because of the high temperature capability and outstanding performance record of this material. The unmodified alloy has only a moderately favorable figure of merit. However, work that has been done on the effect of adding GaP to decrease thermal conductivity and thereby increase the figure of merit has shown great promise that the goal of 9% modular efficiency for the SiGe-GaP modules appears attainable. The module development program is directed towards obtaining the highest possible figures of merit from the SiGe-GaP system, minimizing parameter losses occurring in module construction and demonstrating long-term constancy of output under high-power-density operation.

The radiator design features potassium heat pipes that are longer (5 to 6 m) than any that have been tested. Hence, the development program includes performance verification testing of these pipes as well as long-term reliability testing. A number of fabrication alternatives are available and work will be done to select the most suitable of these. Alternative methods of armoring the radiator heat pipes are being investigated in a subprogram that includes experimental determination of the resistance of lightweight armor materials to hypervelocity impact.

The prime candidate for fuel is UO_2-20 vol% Mo. UO_2 has been used extensively in other reactors. The major new development is in the core configuration. The probability of successfully designing the core with this fuel is considered high.

Core heat pipe development depends on learning to bend high-temperature heat pipes without loss of wick attachment and manufacturing fine mesh molybdenum screen material. Straight molybdenum heat pipes have a good history of operating at the temperatures of interest. The degree of bending required depends on whether the core heat pipes are routed to the thermoelectric converters through the shield or around the shield. Arterial wick configurations, despite increased fabrication complexity, have significant operational advantages that make them the design of choice.

Developing confidence that components will meet the lifetime of interest presents a major

challenge. Accelerated component demonstration testing will be performed on the reactor heat pipes, thermoelectrics, and radiator heat pipes. During the development phase, accelerated testing relationships must be found to verify this approach.

Similar relationships will be sought for irradiation tests of fuel segments that will measure the interactions between the fuel and heat pipes in a simulated power plant environment. The effects of radiation and fission product formation on core heat pipe structure and operation need to be determined. These effects are expected to be small, but experimental verification is needed to develop the confidence to proceed to a demonstration power plant.

Overall, we believe that the risks involved in the nuclear power plant are reasonable and that a high degree of confidence exists in demonstrating technical feasibility. Sufficient experimental data should be available by the end of FY-1983 to proceed to a ground demonstration power plant if potential mission requirements warrant. The activities in the present program will result in a relatively modest investment before commitment to the full-scale ground demonstration of a 10-100-kW$_e$ nuclear power plant.

Currently, the component technology program is funded by the DOE at $2 million per year. This level of funding started in FY-79 and is expected to continue for 5 years. Figure 17 is the program plan for the technical feasibility phase now on-going. Depending on mission requirements, the next phase would be to build a ground demonstration of the power plant. The funding for this would be on the order of $15-20M per year.

V. EARLY KEY RESULTS
A. UO_2/Molybdenum Thermal Coupling Analysis

In the layered fuel configuration, reliance is placed on the molybdenum sheets to carry heat from the UO_2 to the heat pipes. Temperature distributions in this fuel are relatively easy to calculate by assuming that the only heat-flow component in the UO_2 is perpendicular to the molybdenum sheets and that the flow path in the molybdenum sheets is radially inward to the heat pipe. This type of analysis has indicated that a four to one ratio of UO_2 to molybdenum would give maximum molybdenum sheet temperatures on the order of 200 K above the heat pipe
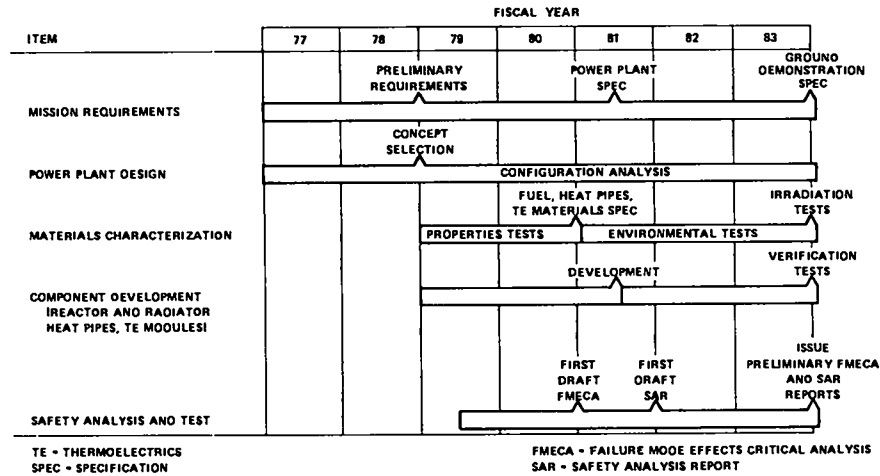
Fig. 17. Program plan.

TE - THERMOELECTRICS
SPEC - SPECIFICATION

FMECA - FAILURE MODE EFFECTS CRITICAL ANALYSIS
SAR - SAFETY ANALYSIS REPORT

temperature for an input power density of 116 MW/m^3 in the UO_2. The maximum temperature in the UO_2 tiles depends on the UO_2 thickness, with the temperature rise to midplane varying from 20 K for a 2-mm tile thickness to 200 K for 6-mm thickness.

The results of this analysis have been confirmed by a more detailed finite element analysis of the molybdenum sheet/UO_2 tile configuration. In this treatment, the thermal contact between the UO_2 tiles and adjacent molybdenum sheets was assumed to be either perfect conductive contact or by radiation only, in which case both surfaces were assumed to have the nominal UO_2 emissivity of 0.8. In addition, the thermal contact of the molybdenum sheets with the heat pipe was varied from 12.5 to 100% of perfect thermal bonding. Table VIII gives calculated temperatures for the case where the inner heat pipe diameter is at a temperature of 1400 K, the power density in the UO_2 is 86.7 MW/m^3 (corresponding to a heat pipe location in the core periphery), and the UO_2 tiles and molybdenum sheets are 1.6 and 0.4 mm thick respectively.

The table indicates that fuel temperatures are not excessive even when the only transfer of heat from the UO_2 to the molybdenum is by radiation and poor contact exists between the molybdenum sheets and heat pipes. The assumption that the molybdenum sheets have the high emissivity of UO_2 is warranted by the rapidity with which UO_2 will coat the molybdenum because of its non-negligible vapor pressure. Table IX lists UO_2 coating times as a function of temperature under the assumption that reevaporation is negligible.

The results in Table IX indicate that establishing good thermal contact between the UO_2 tiles and molybdenum sheets in the layered fuel concept is not a problem because high UO_2 temperatures that occur because of poor contact are self-corrective - rapidly so in terms of establishing a sufficiently thick UO_2 coating (roughly 1 μm) on the molybdenum to produce a high emissivity surface. On a longer-term basis the effective thermal contact will be further improved by the deposition of macroscopically-thick UO_2 layers on the molybdenum sheets. Very poor thermal contact between the molybdenum sheets

TABLE VIII

TEMPERATURE OF LAYERED FUEL CONFIGURATION (K)

	Full	50%	25%	12.5%
Mo sheet/heat pipe contact				
Max. heat pipe temp. exterior wall	1432	1432	1434	1434
Max. Mo sheet temp.	1671	1689	1723	1773
Max. UO_2 interior temp.:				
Radiative transfer	1861	1875	1901	1941
Conductive contact	1708	1725	1759	1809

TABLE IX

UO$_2$ TRANSPORT

Temperature (K)	Vapor Pressure[6] (Pa)	Transport Times (s/μm)	(h/mm)
1400	4.0×10^{-9}	1.4×10^9	3.9×10^8
1600	1.5×10^{-6}	3.9×10^6	1.1×10^6
1700	2.0×10^{-5}	3.1×10^5	8.5×10^4
1800	2.0×10^{-4}	3.2×10^4	8.9×10^3
1900	1.6×10^{-3}	4.1×10^3	1.1×10^3
2000	1.1×10^{-2}	6.4×10^2	1.8×10^2
2100	6.2×10^{-2}	1.1×10^2	3.1×10^1
2200	3.1×10^{-1}	2.3×10^1	6.4

and heat pipes could cause high UO$_2$ temperatures, but, again, this is self correcting because UO$_2$ will deposit quickly around the heat pipe and tend to bridge the area of poor contact.

The analysis that has been done to date has shown the layered fuel form to be even less sensitive to incomplete thermal contact between the core components than had been anticipated. However, it is still necessary to demonstrate that the various methods of achieving thermal contact between the molybdenum sheets and the heat pipes achieve at least 10% of full metallurgical contact. To this end finite element modeling of a sector of the reactor core is being done to determine the material motions and stresses that occur when the core is brought up to operating temperature. Concurrently, experimental measurements of temperature distributions in mock-up assemblies are being made and prototypical molybdenum sheet/heat pipe assemblies are being tested - all directed towards selecting the best method of producing the layered core configuration.

B. Joining of Heat Pipes to Core Support Plate

The basis for supporting the layered core structure is the 6-mm-thick molybdenum core support plate located where the heat pipes leave the core region. This plate must restrain the heat pipes from moving axially when the molybdenum core sheets are pushed on them during core assembly. The following attributes are desirable for the mechanism that attaches the heat pipes to the support plate:

1. It should not change the mechanical properties of the heat pipe wall, such as by reducing its thickness.

2. No welds to the wall should be used because the weld area is embrittled.

3. Weights should be kept to a minimum.

4. It should be flush with both sides of the molybdenum plate so that multifoil and the BeO wafers that bear on the plate are not interfered with.

Various attachment methods are being investigated for heat pipe/support plate junction and most take advantage of the fact that a gas-tight seal is not necessary for these joints. Direct welding of the heat pipes to the support plate is ruled out not only by the embrittlement concern, but also by the restriction of welding access by the neighboring heat pipes. The attachment methods that have been considered are illustrated in Figs. 18 to 21. Some of these have obvious shortcomings. For instance, the modified swage-lok type of fitting shown in Fig. 18 results in a reduction of the heat pipe diameter that could affect the performance of some wick configurations. Initial attempts to make a swage joint with molybdenum nuts led to cracking of the nuts even though all parts were heated to 500 K, well above the ductile-brittle transition temperature of molybdenum, before torque was applied to the nuts. Tantalum nuts were tried and were successful in achieving a firm connection. The castellated nut fastener requires a groove or depression in the heat pipe wall and has been found to give a rather wobbly connection.

The use of a collar brazed or shrink-fit to the heat pipe makes possible the threaded collar and retainer ring fastening methods illustrated in Figs. 18 and 19 respectively. A molybdenum
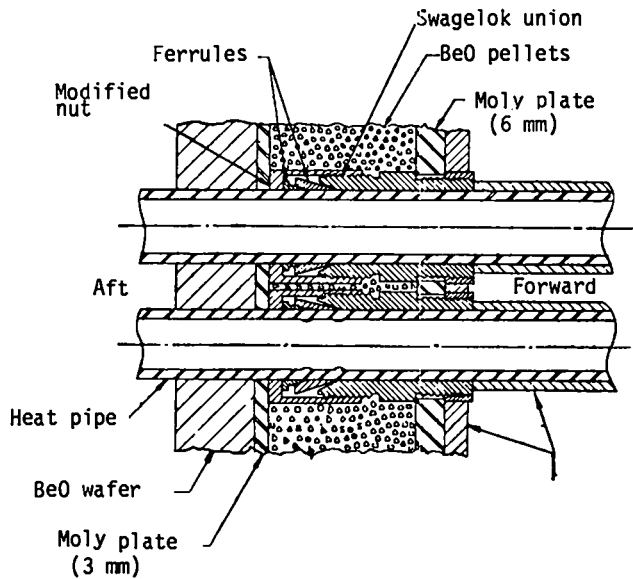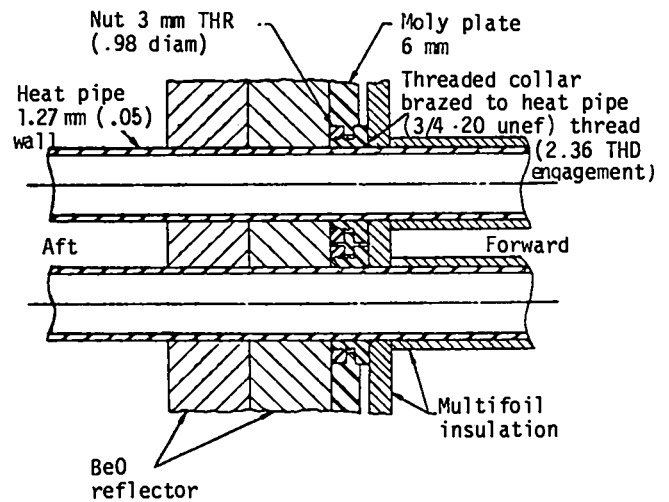
Fig. 18. Modified swagelock type fastener.

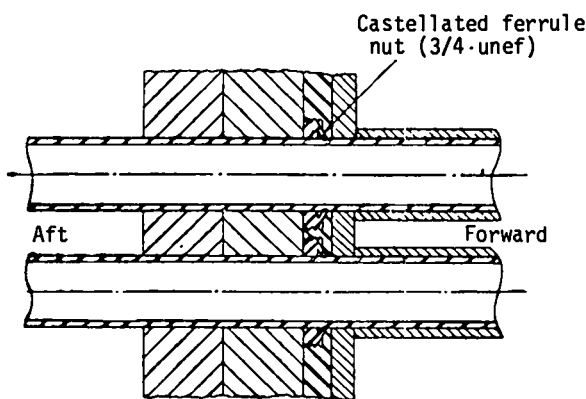Fig. 20. Threaded collar fastener.

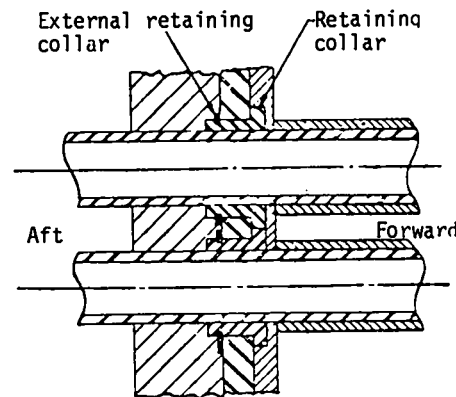Fig. 19. Castellated nut fastener.

Fig. 21. Retainer ring fastener.

collar has been successfully shrunk-fit on to a 15.7-mm-diam molybdenum tube by means of the apparatus shown in Fig. 22. This apparatus holds the collar against a heated support block and aligns the tube as it is rapidly pushed through the collar for a distance of 400 mm. The trial joint was made with a collar having a 0.02-mm interference fit and was able to withstand a force of 100 N without movement. No detectable change occurred in the tube diameter.

The shrink fitting method fits all the criteria enumerated above. It is currently the favored approach for attaching the core heat pipes to the core support plate.

C. Heat Pipe Fabrication

Three types of wick design are being investigated for use in the high-performance core heat pipes. These are shown in Fig. 23.

The screen tube configuration is the most easily fabricated, but lacks pumping redundancy and requires input heat to flow radially inward across the annular working liquid flow channel. This raises the radial temperature drop and also increases the superheating in the liquid returning to the evaporator.

The screen-covered grooved tube is highly redundant in that it retains an adequate performance margin even when several channels become inoperative. However, it also suffers the
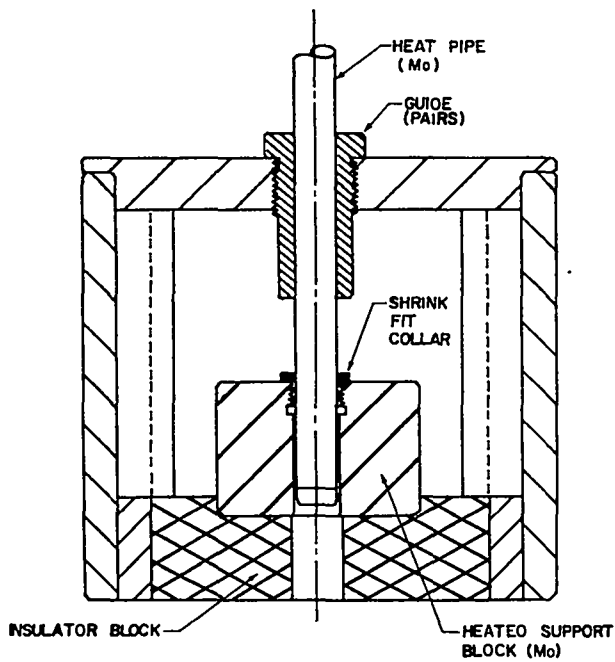
Fig. 22. Fixture for shrink-fitting threaded
collar on molybdenum core heat pipe.

Fig. 23. Potential core-heat-pipe-wick
configuration.

disadvantage of high radial temperature drop and
working fluid superheating and is also difficult to
fabricate.

The multiple artery configuration isolates the
working liquid flow passage from the heat input,
minimizing superheat and radial temperature drop. It
also provides pumping channel redundancy. How-
ever, it involves a complicated fabrication pro-
cedure.

For each of these wick geometries, the pumping
force is provided by the fine porosity of a multi-
layered screen cover. Analysis indicates that suf-
ficient performance margin exists when the effective
pore diameter of the screen is less than 40 μm.
Because such fine pore size is not currently avail-
able in molybdenum screen, several forming tech-
niques are being tried to decrease the pore size of
multiple layers of the finest mesh screen that is
available - 150 mesh with 25 μm wire diameter.
Forming techniques used to compress the screen
layers include ambient temperature pressing between
hardened steel plattens to 242 and 337 MPa, rolling
between stainless steel sheets, and both swaging and
drawing rolls of screen between concentric low car-
bon steel tubes. Acid etching was used to remove
the iron alloy forming or canning material and then
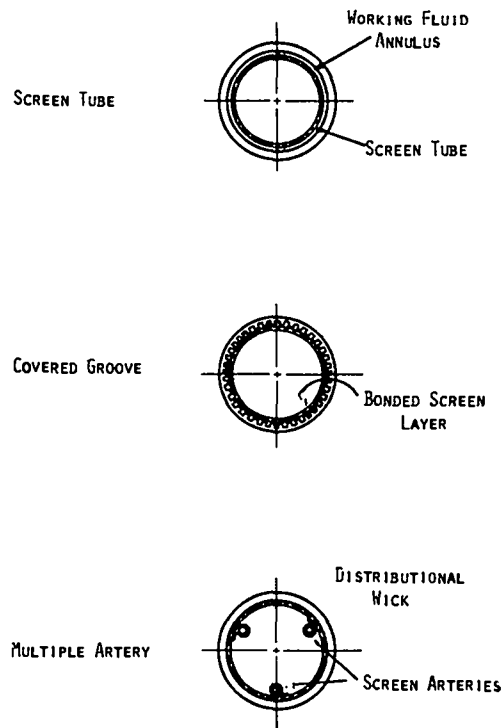the screen specimens were fired to either 1725 or

2025 K in hydrogen for 0.4 to 4 h. Pore diameters
with the various processing techniques ranged from
24 to 80 μm. This compares with the 135 μm pore
diameter of the original screen. Figure 24 shows a
specimen formed between concentric tubes for which
the outer tube was drawn down from 19.0 to 17.9 mm
diameter. The pore diameter achieved for this spec-
imen was 69.5 μm. Attaining finer porosity has been
done at the expense of flow passage density. This
can be seen in Fig. 25, which shows a specimen
formed between concentric tubes by swaging the outer
tube diameter from 19.0 to 12.7 mm. The pore diam-
eter measured by a bubble breakthrough test was
23.6 μm.

It appears that the flow passage density per-
pendicular to the plane of the wick is sufficient
for either annular wick units or arteries but there
is some question whether the density of transverse
flow passages is sufficient for distributional
wicks. Tests are in progress to measure the flow
resistance of these specimens in both directions.

In guaranteeing long life operation of the
molybdenum core heat pipes, it is essential that the
welding required to seal the units - both end cap
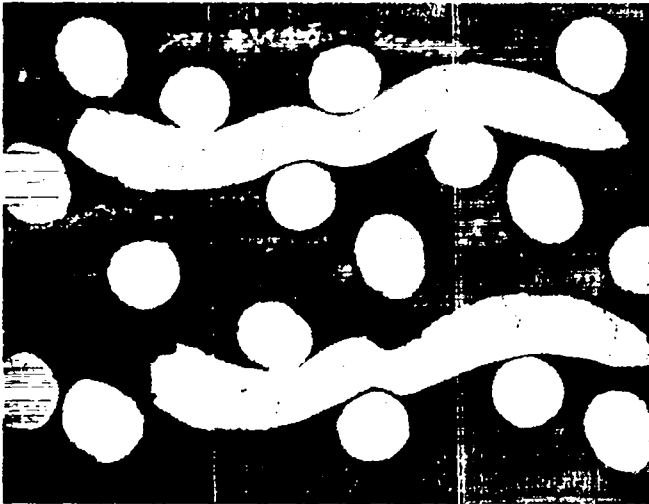and pinch off tube welding - be done so as to give

Fig. 24. Photomicrograph of 150 mesh molybdenum
screen lightly compressed to give a
characteristic pore diameter of 69.5 μm.
Wire diameter is 50 μm.
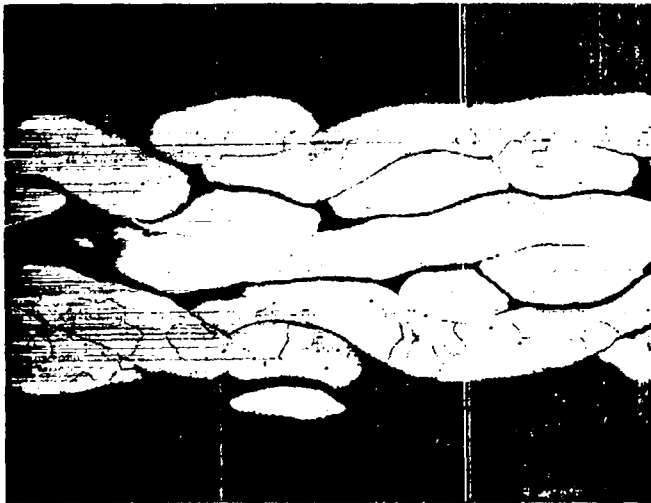

Fig. 25. Photomicrograph of heavily compressed
150 mesh molybdenum screen. Bubble
point pore diameter is 23.6 μm. Initial
wire diameter is 50 μm.

adequate penetration and fine grain size in the weld
zone. This type of weld has been successfully made
for the caps of straight heat pipes with electron
beam welding techniques. However, it is more dif-
ficult to apply this method to the bent heat pipe
configuration required for the SPAR power system.

For this reason, some work has been initiated in
looking at laser and pulsed TIG welding techniques
as alternative heat pipe sealing techniques.

High-repetition rate (> 30 pps) pulsed Nd-YAG
laser welding gives a low heat input that is com-
mensurate with the need for weld zone grain size
control. Trial end cap welds were made with this
method. These were not successful because the maxi-
mum penetration obtained was 1.0 mm for a joint de-
signed for 1.5 mm. As a result, severe underfill
occurred in the weld bead, resulting in extensive
solidification cracking. Revision of the joint de-
sign is in process and further testing of the laser
method as well as trials of the pulsed TIG method
will be made.

Work has been initiated on gauging the compara-
tive effectiveness of laser and electron beam weld-
ing for sealing molybdenum pinch-off tubes. The
specific procedure involves the making of a tempo-
rary seal in a nickel or stainless steel tube that
is attached to the molybdenum tube by a swage con-
nector. A 20-mm length of the 6-mm-diam molybdenum
tube is then raised to a temperature of about 550 K
and flattened in a small portable hydraulic press.
The final seal is made by passing a weld bead across
the flattened portion of the tube. Two laser and
several electron beam trials have been made on spec-
imens of vacuum arc cast molybdenum tubing. Weld
penetration problems again limited the effectiveness
of the laser welding method and weld cracking occur-
red. Less extensive cracking was also observed on
the initial electron beam welded specimens. How-
ever, changing the pre-pinch heat treatment form 1 h
at 1200 K to 1 h at 1700 K has made it possible to
make seal welds free of cracks and leak tight.
Photomicrographs of the seal welds in vacuum arc
cast molybednum and TZM tubes show the latter to
look better, primarily because of small grain size
in the weld bead.

D. Heat Pipe Testing

In the interval required to establish molybdenum
heat pipe fabrication methods and install special
fabrication equipment, work on characterizing the
relative performance of the various types of heat
pipe wick design and determining the effect of bends
in the adiabatic section of the heat pipe has been
done with stainless steel heat pipes with sodium
working fluid. Performance tests of a screen tube

wick geometry have shown general agreement with the analytical predictions. The comparison is shown in Fig. 26 where the axial flow of heat per unit cross-sectional area is plotted as a function of temperature at the exit of the evaporator. The required heat transport from the reactor core of 100 MW/m^2 has been obtained at a temperature more than 200 K below the nominal reactor operating temperature. Measurements were not made at higher temperature for these units because of their stainless steel construction.

Another stainless steel/sodium heat pipe with a screen tube, annular wick geometry was used to investigate superheating limits. This unit was operated vertically with the evaporator at the top so that the working fluid had to flow up a gravity gradient. Under these conditions a wick dryout condition was observed at a temperature of 1200 K and a heat load of 3 KW. This dryout was assumed to be a result of runaway bubble growth in the superheated working fluid in the wick annulus. This growth comes about when a nucleation site is large enough to form a bubble of such size that the expansion force of the net pressure of the vapor within the bubble exceeds the contracting force caused by surface tension. The nucleation site diameter calculated for the observed fryout condition was 4.4 µm. This value was calculated for the heat pipe data given in Fig. 27 and is represented in the figure as a horizontal line. Figure 27 is a plot of the maximum nucleation site diameter that can be tolerated for the annular wick versus the axial heat flux limit of the heat pipe in horizontal operation. It illustrates the effect that, as the heat flux limit of the pipe is increased by operating at ever higher temperatures, the size of the tolerable nucleation site rapidly decreases. Thus, an annular wick heat pipe with the given design parameters is limited to a performance of 8.3 KW and to achieve the desired performance of ⩔ 20 KW the maximum nucleation site diameter must be decreased from 4.4 to 0.2 µm. This can be done in principle by rigorous impurity (notably oxygen) removal methods.

The boiling limit observed in the annular heat pipe is qualitatively different for arterial wicks because the arteries are relatively isolated from the input heat flux. It is anticipated that nucleate boiling in the distribution wick could
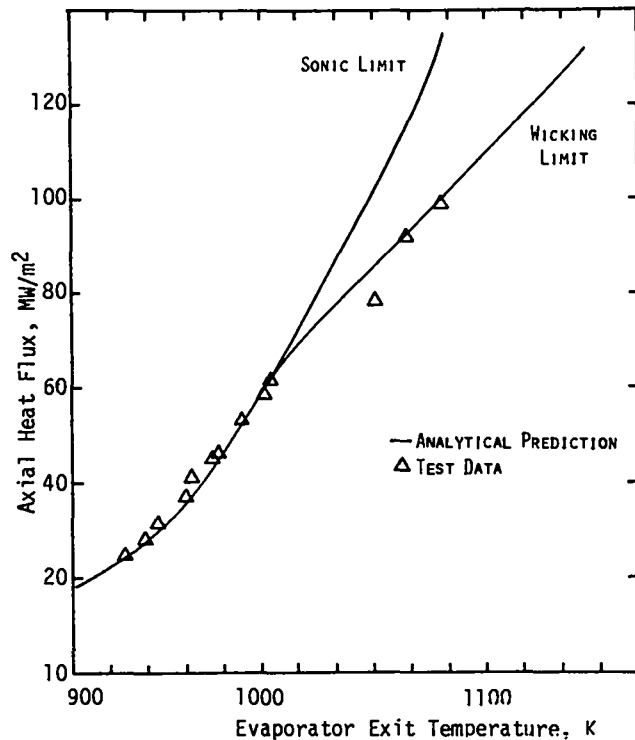

Fig. 26. Heat transport capability versus temperature for sodium heat pipe with screen-tube wick.

eventually occur to such a degree as to interfere with the circumferential flow of liquid through the wick. This phenomenon is expected to occur at much higher values of heat flux than those required for the SPAR application.

Quantitative measurements of bend effects have not as yet been completed. However, a screen-covered grooved tube with two 90° bends on a 180 mm radius has been operated (in air) to 1100 K at a transmitted power density of about 4 kW/cm^2 - which was all that was expected for this unit based on measurements made prior to bending. This unit is shown in Fig. 28.

Although life testing of the SPAR core heat pipes with sodium working fluid is yet to commence, related data is being obtained on a molybdenum/lithium heat pipe that is being tested at 1700 K, 300 K higher than the SPAR heat pipe temperature. This unit was fabricated from low carbon, vacuum arc cast molybdenum. It contains 2 g of hafnium getter. Strips of high purity power metallurgy molybdenum are imbedded in the molybdenum wick for comparative studies. It has
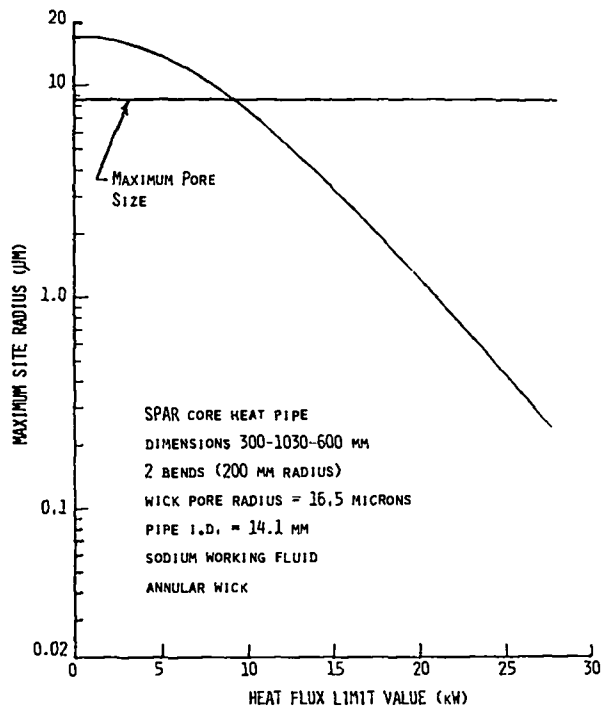
Fig. 27. Maximum tolerable nucleation site radius. for various values of the axial heat flux limit.
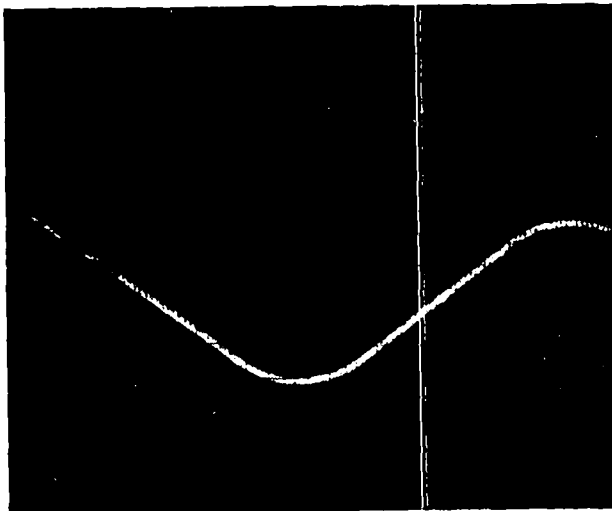

Fig. 28. Stainless steel heat pipe with sodium working fluid operating in air at 1100 K.

successfully withstood 78 cycles from ambient to full operating temperatures (1700 K) while accumulating 15 200 test hours.

E. Thermoelectric Material Development

Silicon-germanium alloys not only posses. attractive thermoelectric performance characteristics but also have mechanical and physical attributes that make them highly desirable candidates for space power applications. Most important of these is their stable high-temperature operating capability, because this allows higher cold-side temperatures and, hence, reduces the radiator weight of space power supplies.

The attractiveness of SiGe alloys exists despite a relatively simple lattice structure that results in thermal conductivity values considerably higher than other common thermoelectric materials and lower peak values of the figure of merit. Obviously then, a method of decreasing the thermal conductivity without changing the other physical properties that determine the figure of merit, namely the Seebeck coefficient and electrical resistivity, would yield a material of higher intrinsic efficiency. A promising approach for accomplishing such a result is to use cross-doping with Group III-V compounds to reduce the thermal conductivity of SiGe by increasing the complexity of its lattice structure. This approach is being pursued as part of the SPAR program.

The development of the cross-doping approach has been directed specifically at investigating the effect on the figure of merit of small additions of GaP to n-type 80 at.% Si - 20 at.% Ge. Specimens of this GaP-modified SiGe alloy were produced by hot pressing methods and considerable effort was devoted to optimizing fabrication parameters. Among the parameters investigated were average particle size of the starting powder, pressing temperature and pressing time.

The investigation of the effect of starting powder particle size extended over a range of 50 to 200 mesh for a 5% GaP molar concentration. Pressing parameters were 180 MPa pressure, a temperature of 1550 K and a pressing time of 1.0 h. Measurements of electrical resistivity and Seebeck coefficient over the range of 400-1000 K showed very little difference for the various starting particle sizes. The main effect was decreasing thermal conductivity with increasing mesh, presumably because the largest mesh (smallest particle size) yielded a more uniform alloy. The figure of merit versus temperature curve for the specimen made with 200 mesh, starting powder is shown in Fig. 29. This represents the best performance obtained with the 5 mole percent GaP addition.

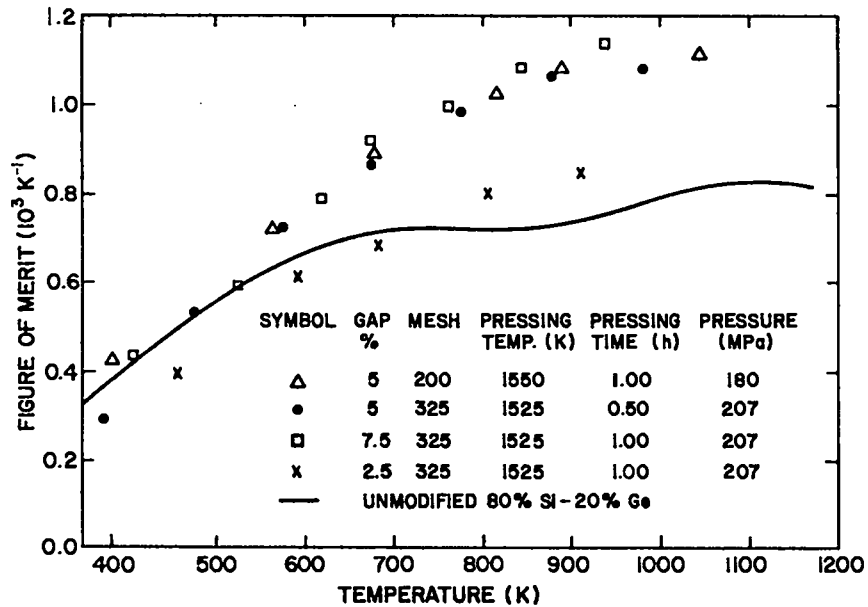The variation of pressing temperatures was done for a series of specimens with 5 mole percent GaP

Fig. 29. Effect of GaP content on figure of merit of n-type SiGe alloy.

that were pressed at 207 MPa for 0.5 h. The start-
ing powder particle size was chosen to be 325 mesh
for this series and pressing temperatures were 1395,
1460, 1525 and 1600 K. The electrical resistivity,
thermal conductivity, and Seebeck coefficient of
these n-type specimens were measured as before over
the 400-1000 K temperature range.

This investigation showed that the figure of
merit was largest for the 1525 K pressing temper-
ature, primarily because the thermal conductivity
reached a minimum for this temperature. In order
for the GaP to be effective in decreasing the ther-
mal conductivity, it must alloy uniformly with it.
It is presumed that uniformity was not achieved for
pressing temperatures below 1525 K. The increase in
the thermal conductivity that was observed for the
specimen pressed at 1600 K is believed to result
from loss of GaP occurring during pressing at this
higher temperature.

A study has also been made of the effect of
varying the amount of GaP added to the n-type SiGe
alloy. Specimens containing 2.5 and 7.5 mole per-
cent GaP were prepared by pressing a mixture of 325
mesh powder at 207 MPa for 1 h at 1525 K. Measure-
ments of the figure of merit are recorded in Fig. 29
along with a solid curve giving the temperature de-
pendence of unmodified Si-20 at.% Ge alloy. The
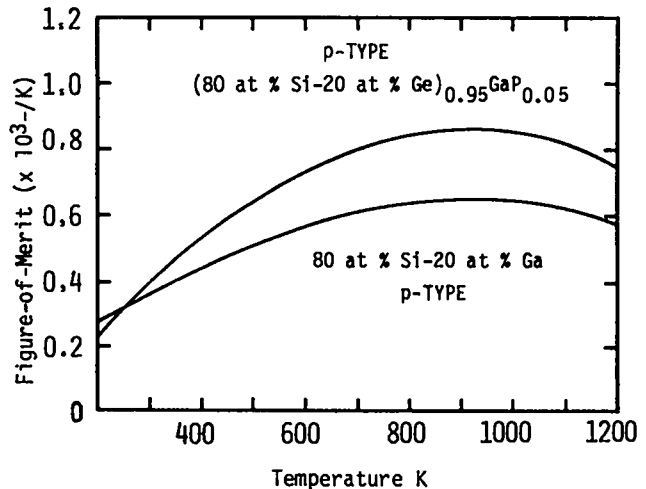2.5% GaP specimen yielded a performance improvement

Fig. 30. Figure of merit vs temperature for
p-type SiGe alloys with and without
GaP additive.

over the unmodified alloy only in the temperature
range above 750 K, whereas the 7.5% GaP specimen
yielded the highest performance observed to date for
SiGe-based alloy. In the temperature range of
750-950 K the increase in the figure of merit is 45%.

Investigations with the GaP additions to p-type
Si-20 at.% Ge alloy have been limited to one run
with 5 mole percent GaP. The figure of merit ob-
tained with this material is compared to that of the
unmodified alloy in Fig. 30. Above 800 K, the cold

side temperature for the SPAR system, the performance improvement is about 30%.

F. Thermoelectric Module Design

The objectives of the thermoelectric module design effort are to achieve high efficiency and low mass. The development of the GaP-modified SiGe alloy is a major step in fulfilling the first of these goals. To achieve the second, the most important step is to aim for high heat flux through the thermoelectric material because the mass of thermoelectric material required to produce a given electrical power output decreases inversely on the square of the power density. The dependence of the module mass on power density is not this strong because the relative mass of the electrical leads increases with increasing power density.

The thermoelectric module illustrated in Fig. 31 is designed for a heat flux of 500 kW/m^2 (50 W/cm^2) entering the hot side of each element of thermoelectric material. This level of heat flux input is easily achieved with the heat pipe that transmits the reactor power to the module. Less easily achieved is the thermal bonding at the interface between insulator, electrical lead, and thermoelectric material that the input heat must traverse in flowing radially through the ring segments of the thermoelectric module.

Thermal contact in the initial test mode of module segments will be achieved by using the outer sleeve of each ring segment to compress the components within, thus establishing pressure contact at the various interfaces. Figure 31 shows the design of the test model of the ring segment. Several of these units will be connected in series to form a fractional length module that will demonstrate the general feasibility of the compression module approach to high power density capability and test the effect of the thermoelectric unit load on the start-up dynamics of the heat pipe. To this end, each ring segment has its own gas gap calorimeter which can provide a close simulation of the coupling heat pipes that will encase the segments of the actual thermoelectric modules. These calorimeters are designed so that they can be installed sequentially on a cluster of closely spaced ring segments. The initial test models will be unmodified Si - 20 at.% Ge alloy thermoelectric material.

The ultimate goal of thermoelectric module development is to move to what is termed an all-bonded unit - where all the interfaces are metallurgically bonded. This approach will reduce parasitic temperature drops at the matrix interfaces to a minimum without the need for contact pressure. Creep analysis, based on silicon creep data, has shown that
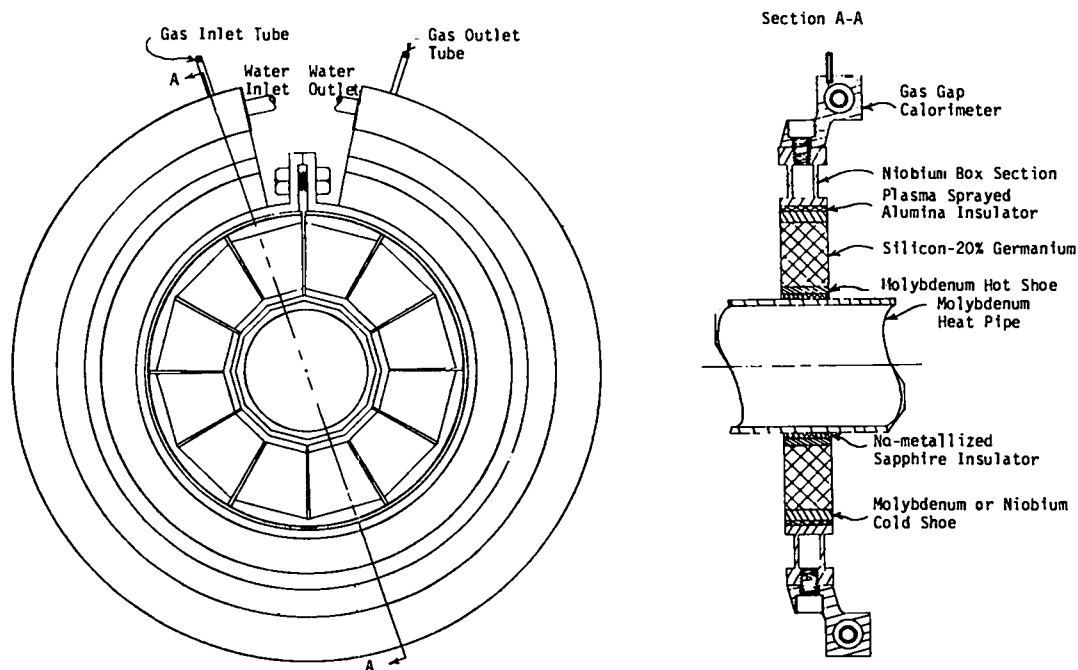

Fig. 31. Thermoelectric submodule with niobium box section and calorimeter.

maintaining interface contact pressures on the order of just a few hundred kilopascals for long periods of time is not feasible.

G. Radiator Heat Pipe Development

Because beryllium was the initial choice as the material for the radiator heat pipes, a limited effort was initiated to determine welding parameters and compatibility with nickel. The latter was of interest in case beryllium and potassium proved to be incompatible as heat pipe materials. Because nickel-potassium heat pipes have been shown to have exceedingly long lifetimes, the use of a thin layer of nickel to line the beryllium might offer a potential fix. The test of beryllium-nickel compatibility involved heating a number of samples of nickel-jacketed beryllium wire in a vacuum furnace for times up to 1373 h in the temperature range of 675 K to 975 K. Reaction layer thicknesses were determined by metallography and used to determine a reaction rate constant that is best expressed by the equation

$$Z^2 = 2.88 \times 10^{-2} \ t \ \exp \frac{-13,370}{T} \quad ,$$

where Z is the layer thickness in mm, t is the time in seconds and T the temperature in Kelvin. This equation predicts a layer thickness about 0.5 mm thick would form between beryllium and nickel in a laminated heat pipe operating for seven years at 775 K. This is excessive.

Welding trials with beryllium were devoted to the problem of putting end caps on a simulated heat pipe. Both pulse TIG welding and electron beam welding methods were used on a total of four specimens. Cracking occurred in each of the trial joints. Preheating to 1035 K somewhat alleviated but did not cure the cracking problem.

The limited amount of work that was devoted to assessing the feasibility of using beryllium confirmed what was already known: that beryllium is a difficult material to work with. The recent rapid cost escalation of tubing of this material made it questionable whether it was economically feasible to use it for radiator heat pipes even if the technical problems could be overcome. This led to the elevation of titanium to the top position among potential radiator materials. Titanium has many good fabrication features, particularly welding, and its use makes possible a wide range of possible radiator heat pipe designs.

The titanium heat pipe development effort is aimed at producing thin wall heat pipes of the artery type illustrated in Fig. 32. This configuration has several advantages, one being the ease with which the arteries can be formed and securely mounted in the same welding operation that form the heat pipe envelope. The design also gives greater flexibility in the choice of a surface. The D-shaped cross section (with the flat side being the radiating surface) minimizes the amount of armor that must be used to protect the heat pipe from meteoroids. Because the armored section is of necessity relatively thick, it will have the strength, even in a flat section, to withstand buckling by atmospheric pressure. In addition the curved portion of the D-shaped cross section is much more resistant to buckling and this is highly desirable because mass minimization considerations make it desirable that its wall thickness be as thin as possible.

The D-shaped configuration also gives greater flexiblity in the choice of the distributive wick that collects the condensed fluid in the condenser section of the heat pipe and transports it to the artery and also dispenses liquid from the artery in the evaporator section. This wick can be thin layers of porous material such as screen, sintered particles or plasma sprayed material. It can also be simply a roughened surface such as made by grooving, knurling, sandblasting, differential etching or embossing. Two governing criteria in forming the distribution wick are that the effective capillary pumping radius in the evaporator be smaller than that of the artery and that this radius be sufficiently small in the condenser to wick the working fluid against gravity to a height greater than the diameter of the heat pipe so that the unit may be tested in a terrestrial environment. The former is the more stringent requirement.

Surface structuring is the favored approach of fabricating the distribution wick because it offers a smaller mass radiator system. Trials have been made with embossing, grooving, cross-grooving and sand blasting titanium sheet. Embossing is favored
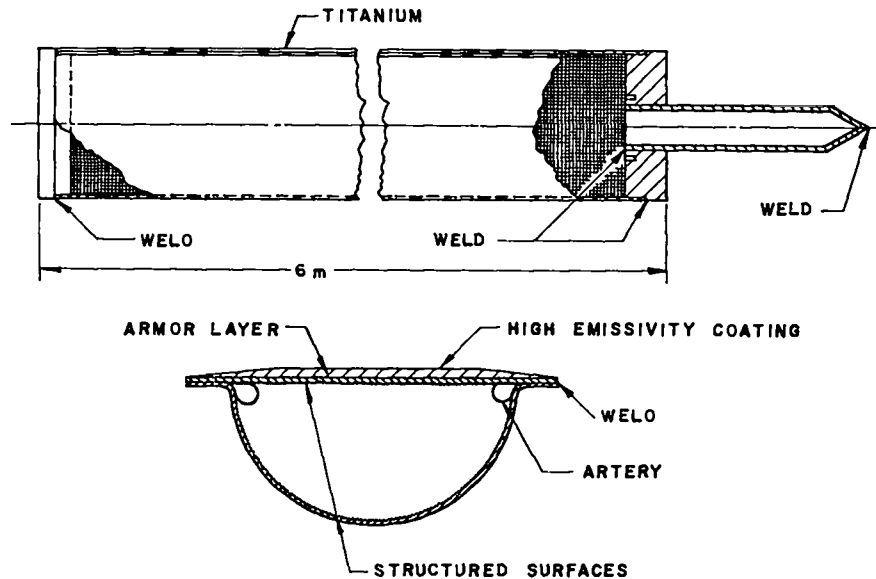
Fig. 32. Radiator type titanium heat pipe.

because of the apparent relative ease with which it can be done. However, the rolling fixture used in the initial attempts was not sufficiently heavy duty to give the desired pattern depth. Grooving and particularly cross-grooving give adequate surfaces, but are expensive to make. Wicking height measurements of sand blasted surfaces indicate they will be quite suitable for distribution wicking. The sand blasting procedure introduces extra stages of cleaning, annealing, and straightening the strips prior to forming and joining them to make the heat pipes. The first trial heat pipes of the D-configuration will use sand blasting and a combination of a sand blasted surface in the condenser and a grooved surface in the much shorter evaporator.

Tests have been initiated at the University of Dayton gas-gun facility to determine the effectiveness of titanium as an armor material. Investigations will include the study of temperature effects, oblique impacts and projective density effects. The work will also include studies of the protective value of coatings of light-weight refractory materials that can be deposited either by plasma spray or other methods to reduce the overall mass increment attributed to armor requirements.

REFERENCES

1. D. Buden, "Missions and Planning for Nuclear Space Power," 14th Intersociety Energy Conversion Engineering Conference, Boston, MA, Aug. 5-10, 1979.

2. R. J. Ackerman, P. W. Gilles, and R. J. Thorn, "High Temperature Thermodynamic Properties of Uranium Dioxide," J. Chem. Phys. 25, 1089-1097 (1956).

3. W. M. Phillips and E. V. Pamlik, "Design Consideration for a Nuclear Electric Propulsion System," 13th Intersociety Energy Conversion Eng. Conf., San Diego, CA, Aug. 1978.

4. W. A. Ranken and D. R. Koenig, "Baseline Design of the Thermoelectric Reactor Space Power System," 14th Intersociety Energy Conversion Conf., Boston, MA, 5-10 Aug. 1979.

5. "Use of Nuclear Power Sources in Outer Space," Working Paper submitted by USA to Committee on the Peaceful Uses of Outer Space Scientific and Technical Subcommittee, Feb. 1979.

6. I. Bekey, A. I. Mayer, and M. G. Wolfe, "Advanced Space Systems Concepts and Their Orbital Support Needs (1980-2000)," Vols. I-IV, Aerospace report ATR-75 (7365)-1, April 1976.

.

.

Microfiche $3.00

001-025	4.00	126-150	7.25	251-275	10.75	376-400	13.00	501-525	15.25
026-050	4.50	151-175	8.00	276-300	11.00	401-425	13.25	526-550	15.50
051-075	5.25	176-200	9.00	301-325	11.75	426-450	14.00	551-575	16.25
076-100	6.00	201-225	9.25	326-350	12.00	451-475	14.50	576-600	16.50
101-125	6.50	226-250	9.50	351-375	12.50	476-500	15.00	601-up	

Note: Add $2.50 for each additional 100-page increment from 601 pages up.